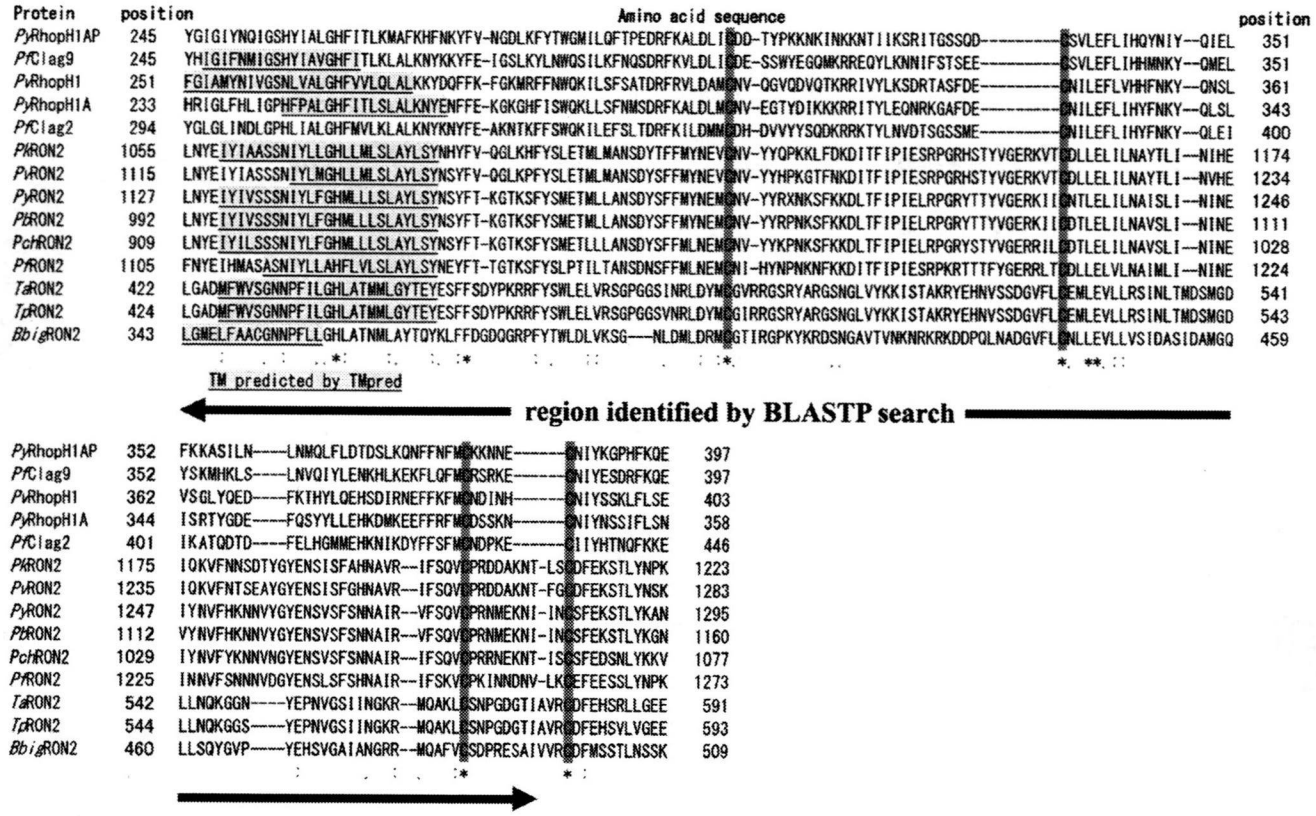

Fig. 2. Amino acid alignment of *Plasmodium* RON2 and RhopH1/Clag. Alignment was generated by MUSCLE [24] with manual correction. "*" indicates that the residues in that column are identical in all sequences in the alignment. ":" indicates conserved substitutions and "." indicates semi-conserved substitutions. In addition to 9 RON2 sequences, *P. falciparum* Clag2 (AAC71977), Clag9 (CAD52032), *P. yoelii* RhopH1A (BAB70675), RhopH1AP (BAB70677), and *Pv*RhopH1 (contig 1047) were used to generate the alignment. Cys residues are highlighted in red. The region possessing homology between RhopH1/Clag and RON2 as identified by BLASTP is indicated by the bar under the alignment.

residues in the cytoplasmic loops of the transmembrane protein [21], which is a likely explanation for this discrepancy.

3.3. *PfRON2 transcription peaks at the schizont stage*

To determine the transcription pattern in the asexual stages of the parasite life-cycle, quantitative RT-PCR was performed on the HB3 parasite line prepared from a synchronized culture harvested at 6 h intervals. Both RON2 and AMA1 transcriptions were seen to peak around 36–40 h after invasion, when parasites were in the schizont stage. AMA1 showed a broader and flatter transcription peak than RON2 (Fig. 3). Transcriptome data compiled in the PlasmoDB website [13,29] also indicated a milder wave crest of AMA1 transcripts compared with RON2.

3.4. *Complex formation of PfRON2, PfRON4, and PfAMA1*

Mouse and rabbit anti-*Pf*RON2 sera were generated using recombinant GST-fRON2N. Firstly, we evaluated the reactivity of anti-*Pf*RON2 sera by Western blot using recombinant proteins. Both antisera recognized the fRON2N component of the recombinant protein after cleavage (Fig. S3, filled arrows). Cleaved 26.4-kDa GST component (Fig. S3, arrowheads) and 46-kDa GST-fused PreScission protease (Fig. S3, unfilled arrow) were also recognized by these Abs.

Secondly, we evaluated the reactivity of these sera against native RON2 proteins extracted from schizont stage *P. falciparum* (HB3 line) by Western blot analysis. Both antisera reacted with a band slightly larger than 250 kDa (Fig. 4A, arrows), which is similar to the predicted molecular weight of *Pf*RON2 after exclusion of the putative signal peptide sequence (247 kDa). An 80-kDa band was detected by both mouse and rabbit antisera in HB3 extract, for which the exact identity is not known, but a possible processed product of *Pf*RON2. A 55-kDa band detected with rabbit antiserum was also detected with preimmune serum, suggesting that this band was unrelated to

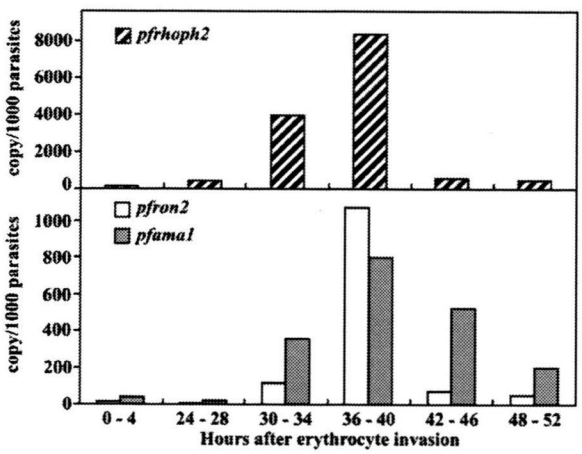

Fig. 3. Transcriptional analysis by quantitative RT-PCR of *pfrhoph2*, *pfron2*, and *pfama1* genes during blood stages of *P. falciparum* (HB3 line). Y-axis indicates copy number of each transcript detected per 1000 parasites. Similar results were observed in 3 independent experiments (data not shown).

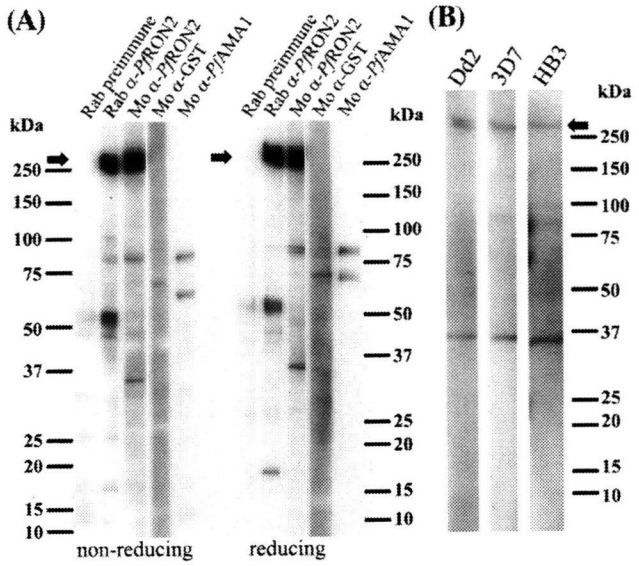

Fig. 4. Western blot analysis of antisera against native parasite proteins. (A) Schizont-enriched parasite extracts were stained by rabbit preimmune serum, (Rab preimmune), rabbit anti-*Pf*RON2 (Rab α-*Pf*RON2), mouse anti-fRON2N (Mo α-*Pf*RON2), and Abs against GST (Mo α-GST) or *Pf*AMA1 (Mo α-*Pf*AMA1) under both reducing and non-reducing conditions. Both mouse and rabbit anti-*Pf*RON2 sera detected a band slightly larger than 250 kDa. (B) Western blot of schizont-enriched parasite extracts from 3 different *P. falciparum* lines, Dd2, 3D7, and HB3 with mouse anti-fRON2N serum. Arrows indicate predicted *Pf*RON2 bands.

*Pf*RON2. A 35-kDa band was detected with mouse antiserum but not with rabbit antiserum, suggesting that it is also unrelated to RON2.

To evaluate the interaction between *Pf*RON2, *Pf*RON4, and *Pf*AMA1, we performed immunoblotting against immunoprecipitated materials from mature schizont-rich parasite extracts (Fig. 5). We found that RON2 was detected in the precipitated fraction using anti-*Pf*AMA1 or anti-*Pf*RON4. In the reciprocal experiment, *Pf*AMA1 and *Pf*RON4 were also detected in the precipitated fraction of anti-*Pf*RON2 serum. Although it is theoretically possible that such immunoprecipitated fractions contained the *Pf*RON2-*Pf*RON4, *Pf*RON2-*Pf*AMA1, and *Pf*RON4-*Pf*AMA1 dimeric complexes as appropriate to the primary

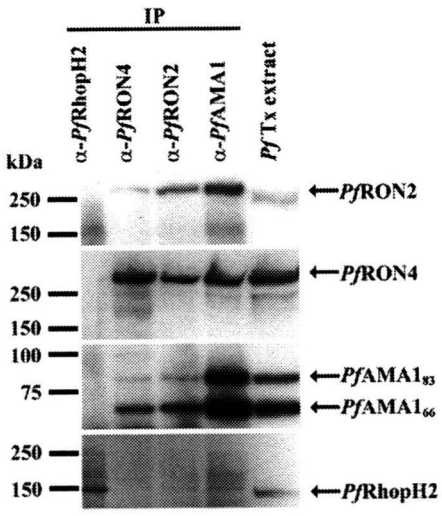

Fig. 5. *Pf*RON2 is co-precipitated with *Pf*RON4 and *Pf*AMA1. Schizont-rich parasite Triton X-100 extracts (*Pf* Tx extract) were immunoprecipitated (IP) with rabbit sera against *Pf*RhopH2 (α-*Pf*RhopH2), *Pf*RON2 (α-*Pf*RON2), *Pf*AMA1 (α-*Pf*AMA1) or mouse monoclonal Ab against *Pf*RON4 (α-*Pf*RON4), then stained against *Pf*RON2, *Pf*AMA1, *Pf*RON4, or *Pf*RhopH2. AMA1$_{83}$ is a proprotein form and AMA1$_{66}$ is a processed form.

antibody, considering that these 3 proteins are distinct molecules that do not possess any similarity each other, this specific co-immunoprecipitation suggests complex formation among *Pf*RON2, *Pf*RON4, and *Pf*AMA1 in *P. falciparum*. The fact that both the 83-kDa proform and the 66-kDa processed form were co-precipitated with *Pf*RON2 indicated that a region responsible for complex formation was located in the 66-kDa form of AMA1 [30]. Neither of these was detected in the anti-RhopH2 immunoprecipitate, thereby excluding not only the possibility of *Pf*RON2 involvement in the RhopH complex, but also potential carryover due to insufficient or inadequate washing steps.

3.5. RON2 is expressed at the rhoptry neck of Plasmodium merozoites

Dual labeling indirect immunofluorescent assay was performed using anti-*Pf*RON2 with either anti-*Pf*AMA1 (microneme marker), anti-Clag3.1 (rhoptry body marker), or anti-*Pf*RON4 (rhoptry neck marker) antibodies in order to determine the sub-cellular location of *Pf*RON2 in *P. falciparum* (Fig. 6). In segmented schizonts, RON2 antisera produced a punctate pattern of fluorescence and each developing merozoite showed a single small punctate *Pf*RON2-positive signal located at the apical end. Although some parts of the *Pf*RON2 signal

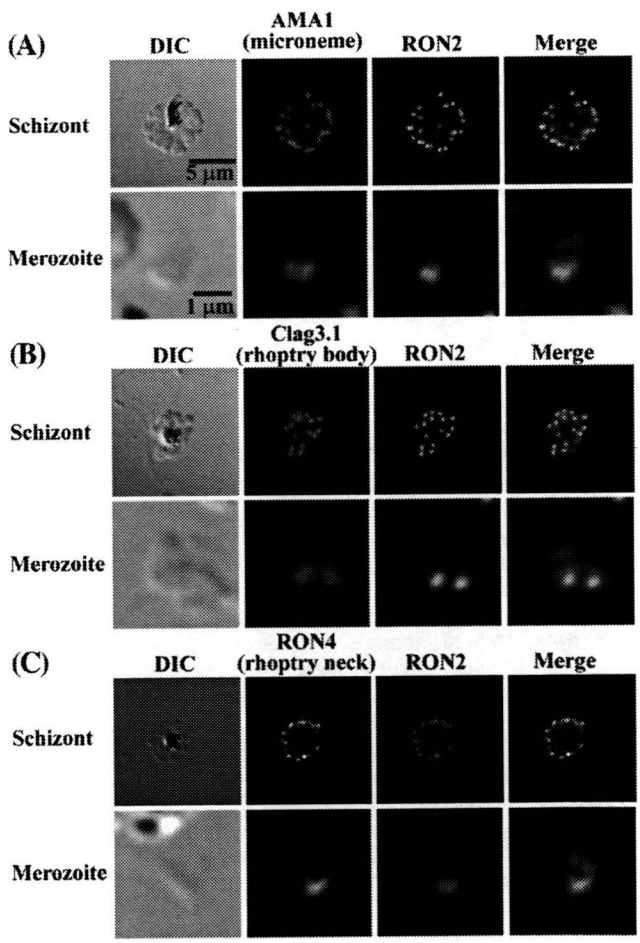

Fig. 6. *Pf*RON2 is expressed at the apical end of *Plasmodium* merozoites. Schizont-infected erythrocytes and merozoites were dual-labeled with antisera against *Pf*RON2 and *Pf*AMA1 (A), *Pf*Clag3.1 (B), or *Pf*RON4 (C). Merged images are shown in the right panels. All segmented schizonts and merozoites are positive for *Pf*RON2. Nuclei are counterstained with DAPI. Colocalization of *Pf*RON2 with *Pf*RON4 (rhoptry neck marker) was observed but neither colocalized with *Pf*Clag3.1 (rhoptry body marker) nor *Pf*AMA1 (microneme marker). To eliminate the background staining, negative control sera were always used and images were assessed (data not shown).

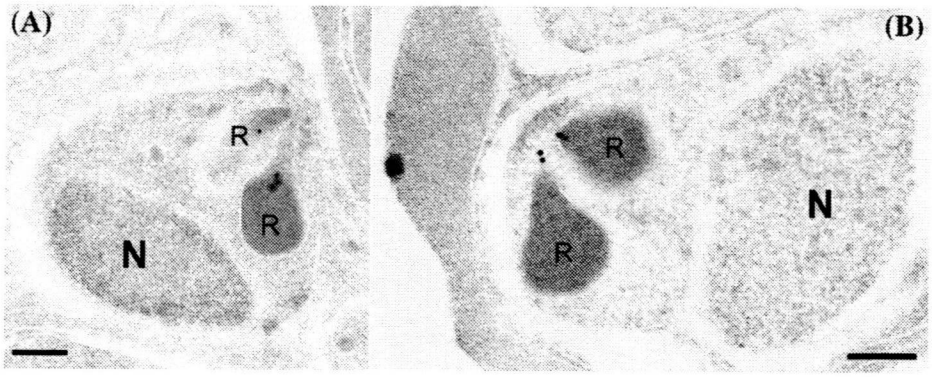

Fig. 7. Rhoptry neck localization of *Pf*RON2 by immunoelectron microscopy. Longitudinally sectioned merozoites in schizont-infected erythrocytes were labeled with anti-*Pf*RON2 serum followed by secondary Ab conjugated with gold particles. Gold particles were restricted to the narrow neck portion of the rhoptries (R). Two different images are shown (A and B). N indicates nucleus. Bars = 200 nm.

overlapped with microneme protein AMA1 and rhoptry body protein Clag3.1, it did not colocalize well with those markers, whereas complete colocalization was observed with the rhoptry neck marker *Pf*RON4.

Immunoelectron microscopy was carried out to determine the precise localization of the protein. *Pf*RON2 was detected in the neck portion of the pear-shaped rhoptries in segmented schizonts (Fig. 7). Thus *Pf*RON2 is seen to compartmentalize in the rhoptry neck.

3.6. Potential positive diversifying selection on *PfRON2*

To evaluate the polymorphic nature of *Pf*RON2, we sequenced the *pfron2* nucleotide sequence (2459–6570), excluding the 5′ low complexity region, in 5 *P. falciparum* parasite lines and compared them with the sequence from the genome database (3D7 line). A total of 5 nonsynonymous nucleotide substitutions were observed at nucleotide positions 2615, 2710, 2914, 4391 and 4392, resulting 4 amino acid substitutions (Table 1). An excess of nonsynonymous substitutions ($d_N = 0.0007 \pm 0.0003$) over synonymous substitutions ($d_S = 0.0002 \pm 0.0002$) was detected ($P = 0.0333$), indicating *Pf*RON2 is subject to positive diversifying selection.

4. Discussion

In this study, we characterized *P. falciparum* RON2 for its protein structure, transcription profiles, intracellular localization, and complex formation with *Pf*RON4 and *Pf*AMA1.

*Pf*RON2 possesses a region harboring homology with another rhoptry protein RhopH1/Clag, a component of the RhopH complex that possesses erythrocyte binding ability [16,31,32]. Co-immunoprecipitation showed that *Pf*RON2 does not form a complex with RhopH2, suggesting that *Pf*RON2 is unlikely to be a component of the RhopH complex. Because RON2 orthologs can be found in other apicomplexan parasites and RhopH1/Clag is found only in *Plasmodium* species, RhopH1/Clag probably evolved via acquisition of a conserved functional domain from RON2 during its generation in *Plasmodium* species. Thus, this homologous region may have a common function between these two complexes. The sequence of *Tg*RON2 deposited to the database (GenBank accession number DQ096563) only possesses the C-terminal half of the conserved region between RON2 and RhopH1/Clag. By comparing *Tg*RON2 gDNA and cDNA sequences, we noticed that intron 3 is relatively large (2272 bp) and contains a potential sequence encoding the N-terminal portion of the conserved region. Thus it is possible that there is another alternatively spliced transcript encoding the full length of the conserved region. Alternatively, it is also possible that this region represents an ancient vestigial exon.

Interestingly, we could readily detect complex formation between AMA1 and RON proteins in the extract obtained from mature schizont-rich parasites, suggesting that complex formation had already occurred at the schizont stage likely at the apical end upon secretion of RON proteins from rhoptry and AMA1 from microneme. This is in contrast to the other apicomplexa parasite *T. gondii*, in which the AMA1-RON complex was proposed to form at the initial contact with the host cell. The precise timing of the complex formation is not clear, but may vary depending on the parasite species. Among RON proteins characterized thus far, only *Tg*RON4 was visualized to locate at the moving junction during cell invasion. Whether *Pf*RON2 and *Pf*RON4 locate at the moving junction and whether the complex remains intact during cell invasion are still need to be clarified. We found that *Pf*RON2 degraded more rapidly than *Pf*RON4 after extraction (Fig. S4), which may explain the previous observation by Alexander et al. (2006), who did not detect *Pf*RON2 in the immunoprecipitant with anti-*Pf*AMA1 Ab [7].

The association between the 83-kDa proform of *Pf*AMA1 with RON proteins raises the possibility that the processing of *Pf*AMA1 from the 83-kDa form to 66-kDa form occurs not only in the microneme, as previously proposed [33], but also on the apical tip of the merozoite after release from the microneme in mature schizonts. If this is the case, it is not clear whether this AMA1 processing occurs after complex formation with RON proteins or is mainly achieved prior to this. However, it is formally possible that disruption of the different intracellular microorganelles during the experimental procedure resulted in an artificial complex formation of *Pf*AMA1 proform, for which further studies are required.

Due to the fact that *P. falciparum* AMA1 exhibits relatively high polymorphism between lines, which is considered to be generated by positive diversifying selection under the human immune pressure, we evaluated the polymorphic nature of *Pf*RON2. Although the level of polymorphism of RON2 is not high, the fact that $d_N > d_S$ suggests that positive diversifying selection does indeed act on RON2. Three types of

Table 1
Nucleotide and amino acid polymorphism of *Pf*RON2

Nucleotide positions (amino acid) [a]	Parasite line					
	3D7	7G8	HB3	Dd2	FVO	D10
2614–2616	tCa (Ser)	tCa (Ser)	tCa (Ser)	tCa (Ser)	tCa (Ser)	tTa (Leu)
2710–2712	Cat (His)	Cat (His)	Cat (His)	Tat (Tyr)	Tat (Tyr)	Tat (Tyr)
2914–2916	Gac (Asp)	Gac (Asp)	Cac (His)	Gac (Asp)	Gac (Asp)	Gac (Asp)
4390–4392	gAA (Glu)	gAA (Glu)	gAC (Asp)	gGC (Gly)	gGC (Gly)	gAA (Glu)

[a] Nucleotide numbering is after the 3D7 line sequence.

amino acid substitutions found at aa 1464 (Asp, Glu, and Gly) suggests that this particular site is under diversifying selection and is possibly to be exposed to host immunity. Thus, *Pf*RON2 not only appears to have an important role in host cell invasion by apicomplexan parasites, but also is a potential target for malaria intervention strategies.

Acknowledgements

We thank N Iyoku for her expertise, I Ling for anti-*Pf*RhopH2 serum, C Long for anti-*Pf*AMA1 serum, anti-*Pf*RON4 antibody (26C64F12) for J-F Dubremetz, and R Culleton for critical reading. Preliminary sequence data of *P. knowlesi*, *P. berghei*, *P. chabaudi*, and *B. bigemina* were produced by the corresponding groups at the Sanger Institute website at http://www.sanger.ac.uk/. Preliminary sequence data of *P. vivax* was produced at the Institute for Genomic Research website at http://www.tigr.org. This work was supported in part by Grants-in-Aid for Scientific Research 17590372 and 17406009 (to OK) from the Ministry of Education, Culture, Sports, Science and Technology, Japan. JC acknowledges the support of National Natural Science Foundation of China 30700695.

Appendix A. Supplementary data

Supplementary data associated with this article can be found, in the online version, at doi:10.1016/j.parint.2008.09.005.

References

[1] Snow RW, Guerra CA, Noor AM, Myint HY, Hay SI. The global distribution of clinical episodes of *Plasmodium falciparum* malaria. Nature 2005;434:214–7.
[2] Kaneko O. Erythrocyte invasion: vocabulary and grammar of the *Plasmodium* rhoptry. Parasitol Int 2007;56:255–62.
[3] Aikawa M, Miller LH, Johnson J, Rabbege J. Erythrocyte entry by malarial parasites. a moving junction between erythrocyte and parasite. J Cell Biol 1978;77:72–82.
[4] Boothroyd JC, Dubremetz JF. Kiss and spit: the dual roles of *Toxoplasma* rhoptries. Nat Rev Microbiol 2008;6:79–88.
[5] Alexander DL, Mital J, Ward GE, Bradley P, Boothroyd JC. Identification of the moving junction complex of *Toxoplasma gondii*: a collaboration between distinct secretory organelles. PLoS Pathog 2005;1:e17.
[6] Lebrun M, Michelin A, El Hajj H, Poncet J, Bradley PJ, Vial H, et al. The rhoptry neck protein RON4 re-localizes at the moving junction during *Toxoplasma gondii* invasion. Cell Microbiol 2005;7: 1823–33.
[7] Alexander DL, Arastu-Kapur S, Dubremetz JF, Boothroyd JC. *Plasmodium falciparum* AMA1 binds a rhoptry neck protein homologous to TgRON4, a component of the moving junction in *Toxoplasma gondii*. Eukaryot Cell 2006;5:1169–73.
[8] Baum J, Tonkin CJ, Paul AS, Rug M, Smith BJ, Gould SB, et al. A malaria parasite formin regulates actin polymerization and localizes to the parasite-erythrocyte moving junction during invasion. Cell Host Microbe 2008;3:188–98.
[9] Triglia T, Healer J, Caruana SR, Hodder AN, Anders RF, Crabb BS, et al. Apical membrane antigen 1 plays a central role in erythrocyte invasion by *Plasmodium* species. Mol Microbiol 2000;38:706–18.
[10] Hehl AB, Lekutis C, Grigg ME, Bradley PJ, Dubremetz JF, Ortega-Barria E, et al. *Toxoplasma gondii* homologue of *Plasmodium* apical membrane antigen 1 is involved in invasion of host cells. Infect Immun 2000;68:7078–86.
[11] Mital J, Meissner M, Soldati D, Ward GE. Conditional expression of *Toxoplasma gondii* apical membrane antigen-1 (TgAMA1) demonstrates that TgAMA1 plays a critical role in host cell invasion. Mol Biol Cell 2005;16:4341–9.
[12] Trager W, Jensen JB. Human malaria parasites in continuous culture. Science 1976;193:673–5.
[13] Bahl A, Brunk B, Crabtree J, Fraunholz MJ, Gajria B, Grant GR, et al. PlasmoDB: the *Plasmodium* genome resource. a database integrating experimental and computational data. Nucleic Acids Res 2003;31:212–5.
[14] Tsuboi T, Takeo S, Iriko H, Jin L, Tsuchimochi M, Matsuda S, et al. The wheat germ cell-free based production of malaria proteins for discovery of novel vaccine candidates. Infect Immun 2008;76:1702–8.
[15] Ling IT, Kaneko O, Narum DL, Tsuboi T, Howell S, Taylor HM, et al. Characterisation of the *rhoph2* gene of *Plasmodium falciparum* and *Plasmodium yoelii*. Mol Biochem Parasitol 2003;127:47–57.
[16] Kaneko O, Yim Lim BY, Iriko H, Ling IT, Otsuki H, Grainger M, et al. Apical expression of three RhopH1/Clag proteins as components of the *Plasmodium falciparum* RhopH complex. Mol Biochem Parasitol 2005;143:20–8.
[17] Kaneko O, Fidock DA, Schwartz OM, Miller LH. Disruption of the C-terminal region of EBA-175 in the Dd2/Nm clone of *Plasmodium falciparum* does not affect erythrocyte invasion. Mol Biochem Parasitol 2000;110:135–46.
[18] Torii M, Adams JH, Miller LH, Aikawa M. Release of merozoite dense granules during erythrocyte invasion by *Plasmodium knowlesi*. Infect Immun 1989;57: 3230–3.
[19] Aikawa M, Atkinson CT. Immunoelectron microscopy of parasites. Adv Parasitol 1990;29:151–214.
[20] Bendtsen JD, Nielsen H, von Heijne G, Brunak S. Improved prediction of signal peptides: signalP 3.0. J Mol Biol 2004;340:783–95.
[21] Hofmann K, Stoffel W. TMbase – a database of membrane spanning proteins segments. Biol Chem Hoppe-Seyler 1993;374:166.
[22] Krogh A, Larsson B, von Heijne G, Sonnhammer EL. Predicting transmembrane protein topology with a hidden Markov model: application to complete genomes. J Mol Biol 2001;305:567–80.
[23] Linding R, Russell RB, Neduva V, Gibson TJ. GlobPlot: exploring protein sequences for globularity and disorder. Nucleic Acids Res 2003;31:3701–8.
[24] Edgar RC. MUSCLE: multiple sequence alignment with high accuracy and high throughput. Nucleic Acids Res 2004;32:1792–7.
[25] Tamura K, Dudley J, Nei M, Kumar S. MEGA4: Molecular Evolutionary Genetics Analysis (MEGA) software version 4.0. Mol Biol Evol 2007;24:1596–9.
[26] Altschul SF, Madden TL, Schäffer AA, Zhang J, Zhang Z, Miller W, et al. Gapped BLAST and PSI-BLAST: a new generation of protein database search programs. Nucleic Acids Res 1997;25: 3389–402.
[27] Pain A, Renauld H, Berriman M, Murphy L, Yeats CA, Weir W, et al. Genome of the host-cell transforming parasite *Theileria annulata* compared with *T. parva*. Science 2005;309:131–3.
[28] Gardner MJ, Bishop R, Shah T, de Villiers EP, Carlton JM, Hall N, et al. Genome sequence of *Theileria parva*, a bovine pathogen that transforms lymphocytes. Science 2005;309:134–7.
[29] Le Roch KG, Zhou Y, Blair PL, Grainger M, Moch JK, Haynes JD, et al. Discovery of gene function by expression profiling of the malaria parasite life cycle. Science 2003;301:1503–8.
[30] Howell SA, Withers-Martinez C, Kocken CH, Thomas AW, Blackman MJ. Proteolytic processing and primary structure of *Plasmodium falciparum* apical membrane antigen-1. J Biol Chem 2001;276:31311–20.
[31] Ghoneim A, Kaneko O, Tsuboi T, Torii M. The *Plasmodium falciparum* RhopH2 promoter and first 24 amino acids are sufficient to target proteins to the rhoptries. Parasitol Int 2007;56:31–43.
[32] Rungruang T, Kaneko O, Murakami Y, Tsuboi T, Hamamoto H, Akimitsu N, et al. Erythrocyte surface glycosylphosphatidyl inositol anchored receptor for the malaria parasite. Mol Biochem Parasitol 2005;140:13–21.
[33] Healer J, Triglia T, Hodder AN, Gemmill AW, Cowman AF. Functional analysis of *Plasmodium falciparum* apical membrane antigen 1 utilizing interspecies domains. Infect Immun 2005;73:2444–51.

Parasitology International 58 (2009) 196–199

Contents lists available at ScienceDirect

Parasitology International

journal homepage: www.elsevier.com/locate/parint

Short communication

A small-scale systematic analysis of alternative splicing in *Plasmodium falciparum*

Hideyuki Iriko [a,b,c], Ling Jin [a,b], Osamu Kaneko [d,e], Satoru Takeo [b], Eun-Taek Han [b,f], Mayumi Tachibana [d], Hitoshi Otsuki [d], Motomi Torii [d], Takafumi Tsuboi [a,b,*]

[a] Venture Business Laboratory, Ehime University, Matsuyama, Ehime 790-8577, Japan
[b] Cell-Free Science and Technology Research Center, Ehime University, Matsuyama, Ehime 790-8577, Japan
[c] Department of Microbiology and Pathology, Faculty of Medicine, Tottori University, Yonago, Tottori 683-8503, Japan
[d] Department of Molecular Parasitology, Ehime University Graduate School of Medicine, Toon, Ehime 791-0295, Japan
[e] Department of Protozoology, Institute of Tropical Medicine (NEKKEN), Nagasaki University, Sakamoto, Nagasaki 852-8523, Japan
[f] Department of Parasitology, Kangwon National University College of Medicine, Chunchon 200-701, Republic of Korea

ARTICLE INFO

Article history:
Received 6 November 2008
Received in revised form 30 January 2009
Accepted 15 February 2009
Available online 5 March 2009

Keywords:
Alternative splicing
Exon definition
Gametocyte
Malaria
Plasmodium falciparum

ABSTRACT

During the last decade transcriptome analyses demonstrated that alternative splicing plays an important role to generate a large number of mRNA and protein isoforms from a limited number of genes. However, the frequency of the alternative splicing dramatically varies among living organisms. For example, 35–65% of human genes are involved in alternative splicing, whereas only a few are reported for unicellular organism yeast. Alternative splicing has been observed for several genes in the deadliest malaria parasite *Plasmodium falciparum*, but the frequency and the type were not systematically analyzed so far. In this study, we determined partial cDNA sequences for 88 open reading frames surrounding 246 introns in *P. falciparum* which were transcribed at schizont and gametocyte stages, and observed 15 instances of alternative splicing within a total of 14 gene transcripts, 16% of the analyzed genes. Among 5 basic splicing patterns, alternative 5′ and 3′ splicing, and intron retention were detected. Alternative splicing in 7 open reading frames had effects on the domain architectures of the gene products, which might result in modifying the cellular localization and function of these products.

Malaria is a significant human disease of global concern that causes several million deaths annually, as well as hundreds of millions of episodes of clinical illness. The intricate life cycle of the pathogenic protozoan agent of malaria, *Plasmodium*, belays an extraordinary biological complexity that underlies its development in both a warm-blooded host and mosquito vector. The parasite has the capacity to recognize and infect multiple cell types, such as salivary glands, hepatocytes, and erythrocytes; and has three distinct motile or invasive stages that traverse different tissues before infecting a new host cell [1]. In comparison to the simple unicellular yeasts, which are predicted to have ~5000 genes [2], the estimated size of the *Plasmodium* genome appears to inadequately reflect the remarkable biological complexity of its life cycle. The *Plasmodium falciparum* genome is estimated to have ~6000 genes, and the complexity of unique genes is considerably less due to the amplification of numerous multi-gene families, such as *var*, *rif*, and *stevor* [3], that occupy a significant part of the *Plasmodium* genome.

During the last decade transcriptome analyses demonstrated that alternative splicing plays an important role to generate a large number of mRNA and protein isoforms from a limited number of genes [4,5]. However, the frequency of the alternative splicing dramatically varies among living organisms. For example, 35–65% of human genes are involved in alternative splicing, whereas only a few are reported for yeast [4], despite the observation of 4730 predicted introns that are encoded within *Schizosaccharomyces pombe* genes [2]. In *P. falciparum*, 7406 introns were predicted in the genome, whereas alternative splicing has been observed only for a few genes that might affect protein function. For example, adenylyl cyclase variant isoforms may have functional differences [6]; and MAEBL variant isoforms are suggested to change the type I membrane product to a soluble isoform [7]. Another example is the stromal-processing peptidase and delta-aminolevulinic acid dehydratase, which share a common apicoplast-targeting leader sequence via the skipping of 4 intervening exons [8]. Alternative splicing was also reported for the blood stage antigen 41-3 precursor [9]; CDK-related protein kinase 6 [10]; and an aspartyl protease [11]. Thus, alternative splicing does occur in *Plasmodium*; however, the information is largely anecdotal and the prevalence of this mechanism remains unclear. Since alternative splicing can profoundly affect estimations of the breadth and complexity of the proteome (mRNA sequences) from the genome nucleotide sequence information, algorithms predictive of alternative splicing are increasingly needed. Indeed, we have observed in *P. falciparum* that alternatively spliced transcripts are not as rare as the anecdotal evidence would suggest, in the course of our experiences performing high-throughput cloning of protein expression constructs using cDNA templates [12]. In this report, we summarize our data and

Abbreviations: ORF, open reading frame.

* Corresponding author. Venture Business Laboratory, Ehime University, Matsuyama, Ehime 790-8577, Japan. Tel.: +81 89 927 8277; fax: +81 89 927 9941.
E-mail address: tsuboi@ccr.ehime-u.ac.jp (T. Tsuboi).

1383-5769/$ - see front matter © 2009 Elsevier Ireland Ltd. All rights reserved.
doi:10.1016/j.parint.2009.02.002

assess the frequency and the type of alternative splicing in *P. falciparum*; and predict the effect of altered transcripts on the localization and function of the produced proteins. Moreover, we provide evidence that the protozoan *P. falciparum* possesses both exon- and intron-recognition systems that initiate intron splicing.

The *P. falciparum* NF54 line was maintained in culture as described [13]. Asynchronous parasites were collected, and the erythrocytes were removed by saponin-mediated lysis. Parasite pellets were washed with phosphate buffered saline, and stored at −80 °C until use. Gametocyte stages were induced by maintaining parasite cultures at 37 °C using a gas mixture (90% N_2, 5% O_2, and 5% CO_2) for an extended period of time without the addition of fresh erythrocytes, and fully matured gametocytes were collected, washed in phosphate buffered saline, and stored at −80 °C until use. Sixty-nine % of the parasites were fully matured stage V gametocytes. Total RNA was extracted from parasite pellets using the RNeasy mini kit (Qiagen, Valencia, CA), and RNA preparations were extensively treated with DNase I to remove contaminating DNA. cDNA was prepared using Superscript III reverse-transcriptase (RT; Invitrogen, Carlsbad, CA). Open reading frames (ORFs) transcribed at schizont and gametocyte stages were selected for the analysis based on the transcriptome analysis [14]. Oligonucleotide primers were designed based upon annotated sequences in PlasmoDB [15], in order to PCR amplify predicted full-length ORFs. Eighty-eight ORFs were amplified by RT-PCR and cloned into the pCR2.1-TOPO TA plasmid (Invitrogen). Nucleotide sequence of the inserts were determined for 2 to 8 clones for each ORF using an ABI PRISM® 310 and 3100 Genetic Analyzers (Applied Biosystems, Foster City, CA) with M13(-20) and M13 reverse primers.

In this manner we randomly determined partial cDNA sequences for 88 ORFs surrounding 246 introns. The distribution of the ORFs arranged according to stage-specificity of the transcriptional cluster [14] and the number of the constituent introns are described in greater detail in Table 1. Similar to most other eukaryotes, exon boundaries of *Plasmodium* are demarcated by consensus donor and acceptor splicing junctions, GU and AG, respectively [16]. We observed 15 instances of alternative splicing within a total of 14 gene transcripts, 16% of the analyzed 88 genes (Table 1 and Supplementary Table 1). Because we only sequenced 2 to 8 clones for each intron, this value should be taken as a minimal estimation, and the true frequency of the alternative splicing is expected to be higher. To evaluate the alternative splicing in other strain, we performed RT-PCR analysis using gametocyte pellet purified from a malaria patient blood obtained from malaria endemic area in Mae Sot, Thailand. We checked 7 genes specifically expressed at gametocyte stage (PFE0220w, MAL8P1.149, MAL13P1.85, MAL13P1.211, PFD0700c, PF13_0220, and PFE0680w). As a result, five genes (PFE0220w, MAL8P1.149, MAL13P1.85, PFD0700c, and PF13_0220) also showed alternatively spliced variants together with the predicted parent transcripts as NF54 (data not shown). These results suggest that alternative splicing also occur in naturally isolated *P. falciparum* parasites. It was shown that alternative splicing in *P. falciparum* is a higher level than expected, based on the rarity of alternative splicing events in *S. pombe* [4].

The observed alternative splicing events were classified into 3 types: alternative 5′ splicing (46.7% of cases); alternative 3′ splicing (26.7% of cases); and intron retention/creation (26.7% of cases) (Fig. 1A). Notably, this is the first evidence of alternative 5′ splicing in *P. falciparum*. Another type of alternative splicing is exon skipping, which is the most prominent splicing pattern in metazoans; for example, 38% of events in humans are due to exon skipping [4,5]. Although 3 cases of exon skipping have been reported in *P. falciparum* [6,8,9], we did not observe this type occurring in this study.

Table 1
Analyzed *Plasmodium falciparum* introns in this study.

Cluster[a]	Stage[b]	Total		Alternative splicing	
		ORFs	Introns	ORFs (%)	Introns (%)
3	Gm	42	160	8 (19.0%)	9 (6.0%)
4	R/Sch/Mz	16	18	2 (12.5%)	2 (11.8%)
13	Sch/Gm	2	2	0 (0.0%)	0 (0.0%)
14	Spz/Sch/Gm	6	13	2 (33.3%)	2 (15.4%)
15	Sch	22	53	2 (9.1%)	2 (3.8%)
Total		88	246	14 (16.0%)	15 (6.4%)

[a] Open reading frames (ORF) were clustered based on the transcription pattern [14].
[b] Gm, gametocyte; R, ring; Sch, schizont; Mz, merozoite; Spz, sporozoite.

To assess the effect of the predicted alternative protein products, we analyzed the domain architectures of the splicing variants. Alternative splicing in 7 ORFs (MAL13P1.211, PFE0220w, PF13_0220, PF10_0021, PFD0700c, PF14_0694, and PFI0110c) had effects on the domain architectures of the gene products (Fig. 1B). The predicted parent transcripts (type 1) of MAL13P1.211 and PFE0220w encode proteins which possess a single transmembrane domain at their C-termini; whereas the alternatively spliced products harbored a frameshift and an early stop codon that resulted in truncated proteins lacking transmembrane domains. The cellular localization is therefore likely to depend on the splicing status, and the presence or absence of a transmembrane domain. Other transcripts (type 1) corresponding to PFD0700c, PF14_0694, and PFI0110c possessed at their C-termini an RNA recognition motif, thioredoxin motif, and protein kinase domain, respectively; whereas alternatively spliced variants (type 2) lacked these domains either partially or completely, suggesting that the protein functions would be abolished or suppressed. Although no known functional domains were detected for PF13_0220 or PF10_0021, the type 2 transcripts encode stop codons approximately 20 to 30 amino acids from the start codon, indicating that their expression as mature forms would be abolished.

Interestingly, among the two types of transcripts showing 5′ alternative splicing in *P. falciparum* the transcripts that encoded truncated product (type 2) almost always possessed a splicing site at the 5′ side compared to the predicted parent transcripts (type 1). This suggests that splicing site at 3′ side is original and that a cryptic splice site was activated in the preceding exon, likely weak splicing signal of the original site. In unicellular eukaryote yeast, mutations in splice sites lead to the activation of cryptic splice sites located downstream of the mutated site, suggesting that splicing machineries initially recognize intron (intron definition) [17]. However, in the metazoans, mutations in splice sites typically lead to the activation of cryptic splice sites located in the preceding exon or exon skipping [18], suggesting that the exon is primarily recognized (exon definition). Thus the pattern observed for *P. falciparum* fits to the "exon definition". Furthermore, 3 cases of exon skipping reported in *P. falciparum* support the presence of the "exon definition" system in this protist [6,8,9]. Because the observed intron retentions suggest the presence of "intron definition" system, *P. falciparum* appears to initiate splicing via both "exon definition" and "intron definition" systems. This is similar to the metazoan, *Drosophila melanogaster*, for which both intron retention and exon skipping have been observed [19,20].

In this study, we found frequent 5′ alternative splicing, however this type has never been reported in *P. falciparum* despite well over a decade of molecular cloning history of numerous *P. falciparum* genes. This might be explained by our cloning strategy to target gametocyte transcripts rather than asexual stage transcripts (Fig. 1). Because the *Plasmodium* female gametocyte was shown to translationally repress specific mRNA species by forming a complex in the cytoplasm to store mRNA for translation after fertilization [21], there might be a relation between these two observations via mRNA binding proteins. In all eukaryotes, splicing is mediated by a macromolecular spliceosome machinery that consists of small nuclear ribonucleoproteins (snRNPs) and non-snRNP splicing factors with RNA binding motif, including serine–arginine-rich (SR) proteins. Among SR proteins, SF2/ASF shows multiple functions, one of which is to affect alternative splice site selection by antagonizing other SR proteins, such as SC35 and SRp20 [22,23]. SF2/ASF is also reported to associate with ribosomes to stimulate translation [24]. Such concerted regulation of nuclear and

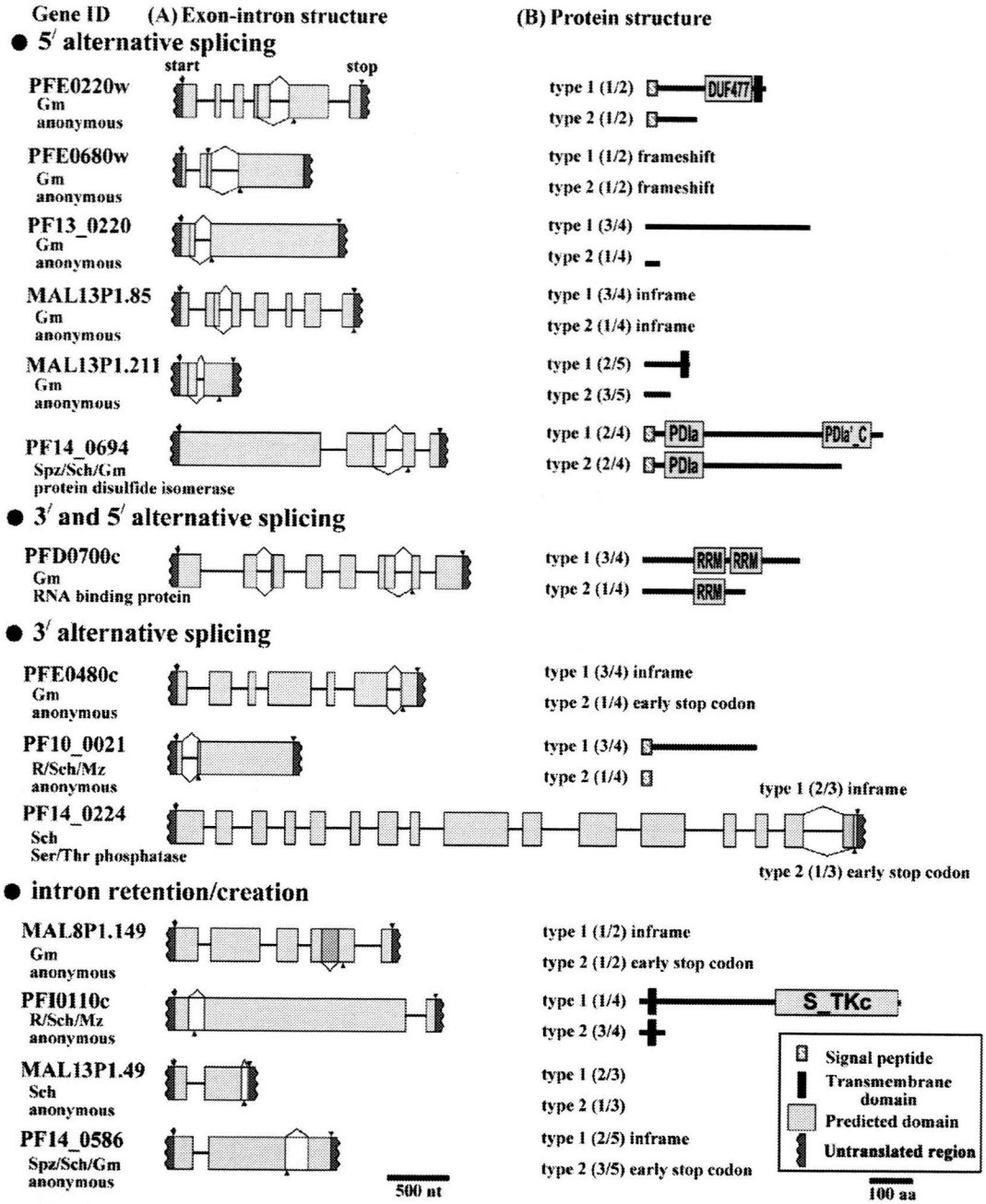

Fig. 1. Alternative splicing events that were detected in this study for *Plasmodium falciparum*. (A) Exon–intron boundaries for 2 types of transcripts are shown. Arrows indicate probable start codons. Arrowheads at the top or the bottom of each schematic indicate probable stop codons according to the exon–intron boundaries. Stage that transcribes each gene is shown under the Gene ID according to the transcriptome analysis [14]; Gm, gametocyte; Sch, schizont; R, ring; Mz, merozoite; Spz, sporozoite. Protein annotations refer to PlasmoDB [15]. (B) Predicted domain architectures of the proteins encoded by two variant transcripts. Type 1 is the presumed original transcript that encodes a longer open reading frame, whereas type 2 encodes a truncated product. The number of the clones for each type, per total clones, is shown in parentheses. Signal peptides and transmembrane domains were predicted by the SignalP and TMHMM2 programs, respectively. Domains were predicted by the SMART program (http://smart.embl-heidelberg.de/) or by searching the Conserved Domain Database (CDD) with Reverse Position Specific BLAST. Domains include: unknown function 477 (DUF477); thioredoxin domain of protein disulfide isomerase family (PDIa); C-terminal thioredoxin domain PDIa′ subfamily (PDIa′_C); Ser/Thr protein kinase motif (S_TKc); and the RNA recognition motif (RRM). The type of alternative splicing for the MAL8P1.149 is likely intron creation rather than intron retention, because type 1 possesses another intron and encoding longer open reading frame.

cytoplasmic activities of SR proteins was shown in mammalian cells [25]. A putative *P. falciparum* ortholog of SF2/ASF (PFE0865c and PF11_0205) might affect alternative splicing in *Plasmodium*. Interestingly, most of the *P. falciparum* genes reported to show alternative splicing are transcribed at the gametocyte and/or sporozoite stages [16], and this observation does not contradict our proposal.

In summary, among 88 isolated genes we found 14 genes that showed alternative splicing patterns, and half of these resulted in an alteration of the protein domain architecture. Splicing machinery initially recognized introns in *P. falciparum*, as suggested by the presence of intron retention, similar to the other unicellular eukaryote yeast. In addition, the pattern of alternative 5′ splicing, in combination with previous reports of the exon skipping, suggests that the exon is also recognized to initiate splicing in *P. falciparum*. This is an important observation, because unicellular eukaryotes are proposed to possess only an "intron definition" system, based on the data from yeast.

Acknowledgements

We thank T. Templeton for critical reading of the manuscript. Gametocyte rich cultures of *Plasmodium falciparum* were a kind gift from C. Long. This work was supported in part by Grants-in-Aid for Scientific Research 18390129 and 19406009 (to T. T.); Scientific Research on Priority Areas 19041053 (to T. T.) from the Ministry of Education, Culture, Sports, Science, and Technology, Japan; and, in part, by a Grant-in-Aid of the Ministry of Health, Labour, and Welfare (H20-Sinkou-ippan-013), Japan (to T. T.).

Appendix A. Supplementary data

Supplementary data associated with this article can be found, in the online version, at doi:10.1016/j.parint.2009.02.002.

References

[1] Markell EK, John DT, Krotoski WA. Medical parasitology. 8th ed. Philadelphia: WB Saunders; 1998.
[2] Wood V, Gwilliam R, Rajandream MA, Lyne M, Lyne R, Stewart A, et al. The genome sequence of *Schizosaccharomyces pombe*. Nature 2002;415:871–80.
[3] Gardner MJ, Hall N, Fung E, White O, Berriman M, Hyman RW, et al. Genome sequence of the human malaria parasite *Plasmodium falciparum*. Nature 2002;419:498–511.
[4] Ast G. How did alternative splicing evolve? Nat Rev Genet 2004;5:773–82.
[5] Stamm S, Ben-Ari S, Rafalska I, Tang Y, Zhang Z, Toiber D, et al. Function of alternative splicing. Gene 2005;344:1–20.
[6] Muhia DK, Swales CA, Eckstein-Ludwig U, Saran S, Polley SD, Kelly JM, et al. Multiple splice variants encode a novel adenylyl cyclase of possible plastid origin expressed in the sexual stage of the malaria parasite *Plasmodium falciparum*. J Biol Chem 2003;278:22014–22.
[7] Singh N, Preiser P, Rénia L, Balu B, Barnwell J, Blair P, et al. Conservation and developmental control of alternative splicing in *maebl* among malaria parasites. J Mol Biol 2004;343:589–99.
[8] van Dooren GG, Su V, D MC, Ombrain, McFadden GI. Processing of an apicoplast leader sequence in *Plasmodium falciparum* and the identification of a putative leader cleavage enzyme. J Biol Chem 2002;277:23612–9.
[9] Knapp B, Nau U, Hundt E, Kupper HA. Demonstration of alternative splicing of a pre-mRNA expressed in the blood stage form of *Plasmodium falciparum*. J Biol Chem 1991;266:7148–54.
[10] Bracchi-Ricard V, Barik S, Delvecchio C, Doerig C, Chakrabarti R, Chakrabarti D. PfPK6, a novel cyclin-dependent kinase/mitogen-activated protein kinase-related protein kinase from *Plasmodium falciparum*. Biochem J 2000;347:255–63.
[11] Volkman SK, Barry AE, Lyons EJ, Nielsen KM, Thomas SM, Choi M, et al. Recent origin of *Plasmodium falciparum* from a single progenitor. Science 2001;293:482–4.
[12] Tsuboi T, Takeo S, Iriko H, Jin L, Tsuchimochi M, Matsuda S, et al. Wheat germ cell-free system-based production of malaria proteins for discovery of novel vaccine candidates. Infect Immun 2008;76:1702–8.
[13] Trager W, Jensen JB. Human malaria parasites in continuous culture. Science 1976;193:673–5.
[14] Le Roch KG, Zhou Y, Blair PL, Grainger M, Moch JK, Haynes JD, et al. Discovery of gene function by expression profiling of the malaria parasite life cycle. Science 2003;301:1503–8.
[15] Bahl A, Brunk B, Crabtree J, Fraunholz MJ, Gajria B, Grant GR, et al. PlasmoDB: the *Plasmodium* genome resource. A database integrating experimental and computational data. Nucleic Acids Res 2003;31:212–5.
[16] Vinkenoog R, Veldhuisen B, Sperança MA, del Portillo HA, Janse C, Waters AP. Comparison of introns in a cdc2-homologous gene within a number of *Plasmodium* species. Mol Biochem Parasitol 1995;71:233–41.
[17] Romfo CM, Alvarez CJ, van Heeckeren WJ, Webb CJ, Wise JA. Evidence for splice site pairing via intron definition in *Schizosaccharomyces pombe*. Mol Cell Biol 2000;20:7955–70.
[18] Berget SM. Exon recognition in vertebrate splicing. J Biol Chem 1995;270:2411–4.
[19] Talerico M, Berget SM. Intron definition in splicing of small *Drosophila* introns. Mol Cell Biol 1994;14:3434–45.
[20] Shen J, Zu K, Cass CL, Beyer AL, Hirsh J. Exon skipping by overexpression of a *Drosophila* heterogeneous nuclear ribonucleoprotein in vivo. Proc Natl Acad Sci USA 1995;92:1822–5.
[21] Mair GR, Braks JA, Garver LS, Wiegant JC, Hall N, Dirks RW, et al. Regulation of sexual development of *Plasmodium* by translational repression. Science 2006;313:667–9.
[22] Jumaa H, Nielsen PJ. The splicing factor SRp20 modifies splicing of its own mRNA and ASF/SF2 antagonizes this regulation. EMBO J 1997;16:5077–85.
[23] Gallego ME, Gattoni R, Stevenin J, Marie J, Expert-Bezancon A. The SR splicing factors ASF/SF2 and SC35 have antagonistic effects on intronic enhancer-dependent splicing of the beta-tropomyosin alternative exon 6A. EMBO J 1997;16:1772–84.
[24] Sanford JR, Gray NK, Beckmann K, Caceres JF. A novel role for shuttling SR proteins in mRNA translation. Genes Dev 2004;18:755–68.
[25] Blaustein M, Pelisch F, Tanos T, Muñoz MJ, Wengier D, Quadrana L, et al. Concerted regulation of nuclear and cytoplasmic activities of SR proteins by AKT. Nat Struct Mol Biol 2005;12:1037–44.

Single amino acid substitution in *Plasmodium yoelii* erythrocyte ligand determines its localization and controls parasite virulence

Hitoshi Otsuki[a], Osamu Kaneko[a,b,1], Amporn Thongkukiatkul[a,c], Mayumi Tachibana[a], Hideyuki Iriko[a,d], Satoru Takeo[e], Takafumi Tsuboi[e], and Motomi Torii[a]

[a]Department of Molecular Parasitology, Ehime University Graduate School of Medicine, Toon, Ehime 791-0295, Japan; [b]Department of Protozoology, Institute of Tropical Medicine (NEKKEN) and the Global Center of Excellence Program, Nagasaki University, Nagasaki, Nagasaki 852-8523, Japan; [c]Department of Biology, Burapha University, Amphur Muang, Chonburi 20131, Thailand; [d]Department of Microbiology and Pathology, Faculty of Medicine, Tottori University, Yonago, Tottori 683-8503, Japan; and [e]Cell-Free Science and Technology Research Center, Ehime University, Matsuyama, Ehime 790-8577, Japan

Edited by Thomas E. Wellems, National Institutes of Health, Bethesda, MD, and approved February 23, 2009 (received for review November 10, 2008)

The major virulence determinant of the rodent malaria parasite, *Plasmodium yoelii*, has remained unresolved since the discovery of the lethal line in the 1970s. Because virulence in this parasite correlates with the ability to invade different types of erythrocytes, we evaluated the potential role of the parasite erythrocyte binding ligand, *Py*EBL. We found 1 amino acid substitution in a domain responsible for intracellular trafficking between the lethal and nonlethal parasite lines and, furthermore, that the intracellular localization of *Py*EBL was distinct between these lines. Genetic modification showed that this substitution was responsible not only for *Py*EBL localization but also the erythrocyte-type invasion preference of the parasite and subsequently its virulence in mice. This previously unrecognized mechanism for altering an invasion phenotype indicates that subtle alterations of a malaria parasite ligand can dramatically affect host–pathogen interactions and malaria virulence.

dense granule | invasion | malaria | microneme | transfection

The rodent malaria parasite *Plasmodium yoelii yoelii* has been widely studied to understand the interactions between the malaria parasite and the host cell (1). The nonlethal 17X line mainly infects young erythrocytes (reticulocytes), whereas the lethal 17XL and YM lines infect a wide range of erythrocytes. These lines have previously been studied to identify the genetic determinants of virulence (2, 3). These differences in erythrocyte invasion preference suggest the possible involvement of a parasite ligand that recognizes erythrocyte surface receptors; however, the actual molecular basis of the observed invasion preference differences remains unclear.

Erythrocyte invasion by the malaria merozoite is a multistep process, initiated by reversible binding to the erythrocyte surface, followed by the establishment of a tight junction between the apical end of the merozoite and erythrocyte surface and the subsequent movement of the merozoite into the nascent parasitophorous vacuole. Each step involves specific interactions between parasite ligands and erythrocyte receptors. Among the ligands of malaria parasites, the best characterized is a type I integral transmembrane protein encoded by the *ebl* (*erythrocyte-binding-like*) gene family. Upon release from the micronemes, EBL proteins recognize erythrocyte receptors and initiate the formation of the tight junction. The importance of EBL in malaria virulence is exemplified in the human malaria parasite *Plasmodium vivax*, which uses an EBL orthologue, *Pv*DBP, to recognize the Duffy antigen on the erythrocyte surface. Because the parasite is apparently unable to use an alternative invasion pathway, individuals in whom the Duffy antigen is not expressed on the erythrocyte surface are completely resistant to *P. vivax* (4, 5). Because of this dramatic association between the disruption of a host–pathogen interaction and protection against a malaria parasite, *Pv*DBP and the *Plasmodium falciparum* EBL orthologue, EBA-175, have been targeted for vaccine development (6).

EBL proteins possess 2 Cys-rich regions conserved among EBL orthologues. The N-terminal Cys-rich region named the DBL (Duffy-binding-like) domain or region 2 (7) recognizes a specific erythrocyte surface receptor. The C-terminal Cys-rich region named the C-cys domain or region 6 is located adjacent to the transmembrane domain, and the number and location of Cys residues are well conserved among known *Plasmodium* species. Region 6 exhibits structural similarity to the KIX-binding domain of the coactivator CREB-binding protein (8) and has been proposed to be a protein trafficking signal for transportation to the micronemes (9). Here we report a single nonsynonymous nucleotide substitution in the *pyebl* gene between lethal and nonlethal lines of *P. yoelii* and show the effect of this substitution on the intracellular localization of EBL, erythrocyte-type preference, and consequently virulence of *P. yoelii*.

Results

To investigate differences in EBL between lethal and nonlethal *P. yoelii* lines, we compared sequences from a variety of malaria parasite species and *P. yoelii* lines 17X, 17XL, and YM. We found 1 nonsynonymous nucleotide substitution in region 6 between the nonlethal 17X and lethal 17XL lines in the entire ORF (Fig. 1). The nonlethal 17X line possesses 8 conserved Cys residues that form 4 disulfide bridges (8), whereas the lethal 17XL line possesses an Arg instead of Cys at the second Cys position. This substitution was also found in another lethal line, "YM" (2), which originated independently from the 17X line during serial passage (3). All *Plasmodium* EBL orthologues for which protein expression was validated possess 8 conserved Cys residues in this region, further indicating that these Cys residues play an important role (supporting information Fig. S1). Thus the observed substitution from Cys to Arg is likely to abolish the native conformation of region 6.

EBL Localizes in the Dense Granules in *P. yoelii* Line 17XL. We raised specific polyclonal and monoclonal antibodies against *Py*EBL

Author contributions: H.O., O.K., and M. Torii designed research; H.O., A.T., M. Tachibana, H.I., and S.T. performed research; T.T. contributed new reagents/analytic tools; H.O., O.K., and M. Torii analyzed data; and H.O. and O.K. wrote the paper.

The authors declare no conflict of interest.

This article is a PNAS Direct Submission.

Data deposition: The data reported in this article have been deposited in the GenBank/European Molecular Biology Laboratory/DNA Data Base in Japan databases (accession nos. AB430781–AB430789).

[1]To whom correspondence should be addressed. E-mail: okaneko@nagasaki-u.ac.jp.

This article contains supporting information online at www.pnas.org/cgi/content/full/0811313106/DCSupplemental.

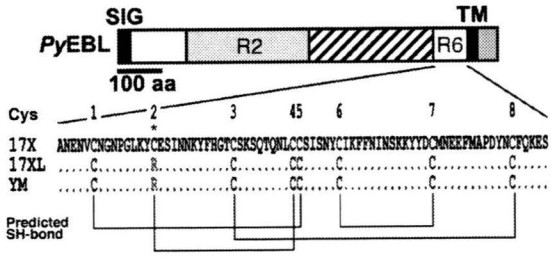

Fig. 1. Schematic structure of *P. yoelii* EBL (*Py*EBL). SIG, TM, R2, and R6 indicate the putative endoplasmic reticulum transporting signal, the transmembrane region, region 2, and region 6, respectively. Amino acid alignment of *Py*EBL from 17X, 17XL, and YM lines are shown below. Eight conserved Cys residues that form disulfide bridges (Predicted SH-bond) and the substitution from Cys to Arg (*) are indicated.

and performed Western blot analysis. The *Py*EBL protein was detected as a 110-kDa band in both the 17X and 17XL lines (Fig. 2*A*). The intracellular localization of *Py*EBL in both the 17X and 17XL lines was compared by indirect immunofluorescent assay

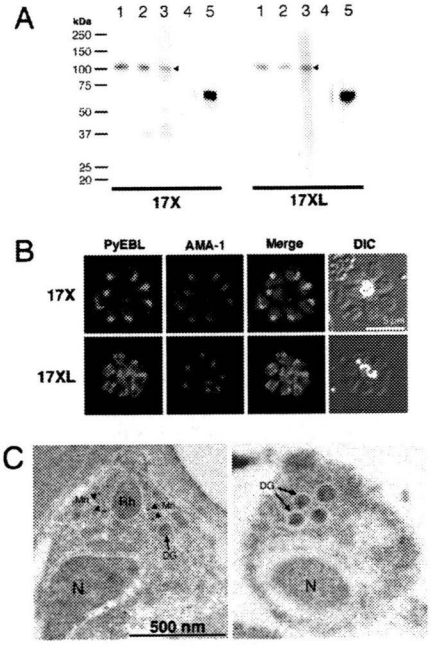

Fig. 2. Western blot analysis and *Py*EBL localization in *P. yoelii* schizont by immunostaining. (*A*) Western blot analysis with mAb 5B10 (lane 1), mAb 1G10 (lanes 2), and mouse serum (lane 3) specific for *Py*EBL against purified *P. yoelii* schizont extracts. A 110-kDa band was detected in both 17X and 17XL lines, with no significant difference in the protein expression level (arrowheads). This band was not detected by normal mouse serum (lane 4). Anti-AMA1 serum detected a 66-kDa band at similar levels (lane 5). (*B*) *P. yoelii* schizonts were incubated with mAb 5B10 (PyEBL), rabbit anti-AMA1 serum (AMA1), and DAPI (blue) for nuclear staining. Schizonts labeled with anti-*Py*EBL (5B10) were stained with FITC secondary antibody (green). Anti-AMA1 were stained with Alexa-546 secondary antibody (red). DIC images are shown in the right-hand column. The 17X line shows apical *Py*EBL signal colocalized with AMA1, but the region 6–substituted 17XL line shows diffused staining that does not colocalize with AMA1. (*C*) Immunoelectron microcopy was carried out for resin-embedded *P. yoelii* 17X and 17XL lines with anti-*Py*EBL mouse serum and secondary antibody conjugated with gold particles. *Py*EBL was detected in the micronemes (arrowheads) of the 17X line, but in the 17XL line it was located in the dense granules (arrows). N, nucleus; Mn, microneme; DG, dense granule; Rh, rhoptry.

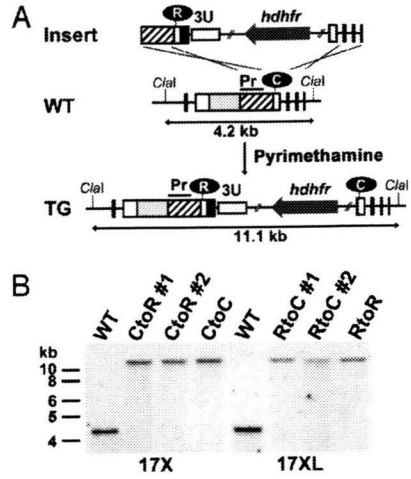

Fig. 3. Amino acid replacement of *Py*EBL region 6 second cysteine location by targeted recombination. (*A*) Schematic representation of the WT and modified (TG) *pyebl* gene loci. The replacement cassette (Insert) was inserted into the *pyebl* gene locus by double-crossover recombination. In this schematic, the second Cys in region 6 was replaced with Arg in the 17X line to generate 17X-CtoR. Other transgenic lines were generated in a similar fashion. ClaI restriction sites and the expected size of the DNA fragment after ClaI digestion are shown. Pr, probe region used in Southern blot analysis. (*B*) Southern blot analysis of the *pyebl* gene locus in WT and transgenic parasite lines derived from *P. yoelii* 17X and 17XL. The absence of the 4.2-kb WT band and the presence of an 11.1-kb band indicate that the *Py*EBL locus was modified in all transgenic clones.

(IFA) using specific antibodies against *Py*EBL (Fig. S2). In the 17X line, *Py*EBL localized to the apical end of each merozoite in both the segmented schizont-stage parasite and individual merozoites, where it colocalized with AMA1, a known microneme protein, under immunofluorescent microscopy (Fig. 2*B*). However, in the 17XL line *Py*EBL did not colocalize with AMA1 at the apical end of merozoites and showed a more diffused but granular distribution in comparison with parasites of the 17X line (Fig. 2*B*). Diffused localization of *Py*EBL was also observed in parasites of the YM line (Fig. S3). Immunoelectron microscopy revealed that *Py*EBL localized in micronemes in the 17X line as reported for *P. falciparum* and *Plasmodium knowlesi* (10, 11). In the 17XL line, however, *Py*EBL localized not in the microneme but in another microorganelle—the dense granules (12) (Fig. 2*C* and Fig. S4).

Because there seems to be only 1 copy of *Py*EBL in the genomes of both lines (Fig. S5), and significant differences were not observed in the level of transcription and protein expression between the 17X and 17XL lines (Fig. 2*A* and Fig. S6), the location of EBL seems to be the most significant difference between them.

Genetic Replacement of Arg and Cys in Region 6 Alters EBL Localization. To evaluate whether the Arg substitution at the second Cys position is responsible for the altered trafficking of *Py*EBL, we exchanged Cys and Arg in the 17X and 17XL lines by genetic modification (17X-CtoR and 17XL-RtoC). The parasites were also transfected with control constructs that do not alter the region 6 amino acid sequence (17X-CtoC and 17XL-RtoR) (Fig. 3*A*). Each of the transgenic parasites was evaluated for the correct integration of the constructs to the *pyebl* gene locus by specific PCR analysis followed by sequencing of the PCR-amplified products (not shown) and Southern blot analysis (Fig. 3*B*).

In the 17X line, replacement of Cys with Arg (17X-CtoR) altered the *Py*EBL localization from an apical pattern to a

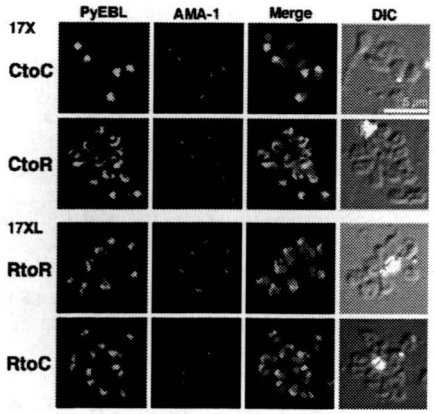

Fig. 4. Replacement of Cys to Arg in region 6 altered subcellular localization of *Py*EBL. Schizonts of transgenic parasite lines were incubated with mAb 5B10 (PyEBL), rabbit anti-AMA1 serum (AMA1), and DAPI (blue) for nuclear staining. DIC images are shown in the right-hand column. In the 17X background, control (CtoC) shows an apical *Py*EBL signal colocalized with AMA1, but replaced (CtoR) shows a 17XL pattern. Inversely, 17XL background control (RtoR) shows a diffused nonapical pattern, but replaced to cysteine (RtoC) shows an apical signal colocalized with AMA1.

nonapical diffused pattern, and *Py*EBL did not colocalize with AMA1. Furthermore, the replacement of Arg with Cys in the 17XL line (17XL-RtoC) altered the *Py*EBL localization from a nonapical diffused pattern to an apical pattern. Control parasites did not display altered *Py*EBL localization (Fig. 4). These results confirm that the observed substitution from Cys to Arg is responsible for the altered localization of *Py*EBL from micronemes to dense granules in the 17XL line.

EBL Localization Alters Erythrocyte-Type Preference and Course of Infection. To determine whether altered localization of *Py*EBL affects erythrocyte-type invasion preference, infected erythrocytes were examined by microscopy, and a selectivity index (SI) was obtained by calculating multiple parasite infection of single erythrocytes for each parasite line on postinfection day 3 in mice (13). We found that 17XL-RtoC predominantly invaded reticulocytes in the same way as the nonlethal 17X line. The SI of the 17XL line (2.38) was increased in 17XL-RtoC ($\approx$35; $P < 0.001$). On the other hand, 17X-CtoR was able to invade a variety of ages of erythrocytes, including mature erythrocytes, comparable to the lethal 17XL line, with the SI of the 17X line (16.78) reduced in 17X-CtoR ($\approx$4; $P < 0.001$; Table 1). These results demonstrate that the localization of *Py*EBL is responsible for the erythrocyte-type preference of the parasite.

Table 1. Selectivity index of WT and transgenic *Plasmodium yoelii* lines

Parasite	*n*	Selectivity index (range)
17X-CtoR 1	5	3.87 (1.86–5.32)
17X-CtoR 2	5	4.25 (2.38–7.97)
17X-CtoC	5	23.53 (16.49–36.00)
17X	5	16.78 (7.60–24.99)
17XL-RtoC 1	5	34.35 (29.18–38.05)
17XL-RtoC 2	5	35.99 (29.97–42.72)
17XL-RtoR	5	1.31 (0.57–2.13)
17XL	5	2.38 (1.58–3.75)

Selectivity indices were calculated from parasitized Giemsa-stained thin blood films collected from each infection.

Because erythrocyte-type preference frequently correlates with virulence in malaria parasites, we further analyzed the transgenic *P. yoelii* parasites for differences in the course of infection and survival of parasite-infected mice. Mice infected with the 17XL-RtoC line developed significantly lower parasitemias compared with the parental 17XL and control 17XL-RtoR lines (Fig. 5*A*), with 100% survival (Fig. 5*C*), whereas all mice infected with 17XL and 17XL-RtoR lines died by day 7 (Fig. 5*C*). The pattern observed for the 17XL-RtoC line was identical to that observed for the nonlethal 17X line. Thus, trafficking of *Py*EBL to the micronemes causes the virulence of the 17XL line to be reduced to the same level as the nonlethal 17X line, suggesting that *Py*EBL is a critical virulence determinant in the 17XL line. The parasitemia of mice infected with 17X-CtoR increased significantly compared with those infected with parental 17X and control 17X-CtoC lines during the acute phase of infection on days 4 to 5 ($P < 0.001$). However, the parasitemia did not reach the level observed for the lethal 17XL line, and it reduced to the same level observed for the 17X and 17X-CtoC lines by day 9 (Fig. 5*B*). No parasites were detectable by microscopy at day 17 (not shown). This suggests that the 17X-CtoR line is able to invade a greater repertoire of erythrocyte types than 17X but is unable to invade as many types as the 17XL line. This reduced capacity to invade multiple erythrocyte types compared with the 17XL line results in a nonlethal infection, in which all mice survive (Fig. 5*C*). Thus, displacement of the EBL from microneme was not sufficient to make this line fully lethal, suggesting the existence of other determinant(s).

Discussion

The results of this study indicate that replacement of Cys to Arg at the second Cys position of *Py*EBL region 6 is the major

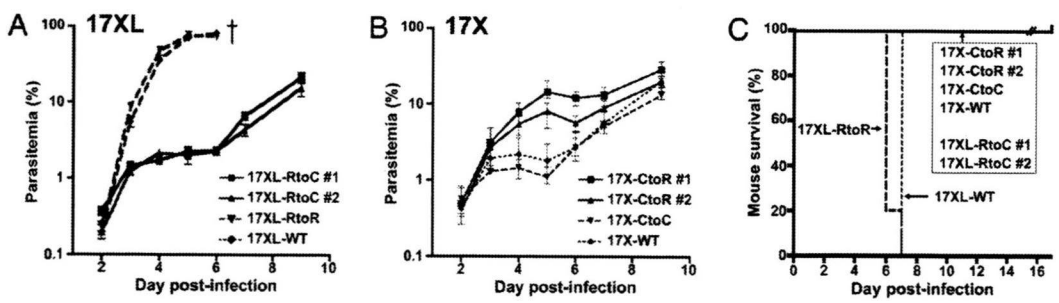

Fig. 5. Effect of the alteration of *pyebl* gene loci on the course of infection and parasite virulence in mice. Mice were i.v. inoculated with 1×10^6 parasitized erythrocytes from WT or transgenic parasite lines. (*A*) Parasitemia of 17XL-RtoC was dramatically reduced to the same level as that of the nonlethal 17X line. (*B*) Parasitemia of 17X-CtoR was significantly higher than parental 17X and control 17X-CtoC on days 4 and 5 ($P < 0.001$), the acute phase of infection; however, the pattern observed is intermediate between the lethal 17XL and nonlethal 17X lines. Parasitemias are plotted using the geometric mean and SD of log-transformed data from groups of 5 mice. (*C*) All mice infected with 17XL-RtoC survived, whereas all mice infected with parental 17XL and control 17XL-RtoR lines died by day 7. All mice infected with 17X, 17X-CtoC, and 17X-CtoR survived.

determinant of the difference between lethal and nonlethal lines of *P. y. yoelii* parasites. This substitution alters the intracellular organelle localization of *Py*EBL from the micronemes to the dense granules and alters the erythrocyte-type invasion preference, course of infection, and parasite virulence in the host.

The crystal structure of region 6 of *P. falciparum* EBA-175 indicates that the second Cys residue forms a disulfide bridge with the fourth Cys residue in this region. Arg substitution of the second Cys residue in the *P. yoelii* 17XL line abolishes this disulfide bridge and thus likely destroys the region 6 structure, which is critical for the trafficking of the protein to the micronemes. It is possible that an incorrectly folded region 6 would not allow the protein to be properly recognized by an (as yet uncharacterized) partner molecule responsible for the trafficking of the EBL protein to the micronemes (9). The mechanism involved in the trafficking of the mutated protein to the dense granules remains unresolved.

Using genetic modification, we have demonstrated that when *Py*EBL is trafficked to the microneme in the 17XL line genetic background, the erythrocyte-type invasion preference and the course of infection are comparable to those of the nonlethal 17X line. This indicates that the substitution of Cys to Arg is a major determinant of the lethal phenotype of the 17XL line. However, when *Py*EBL was not trafficked to the microneme in parasites with the 17X line genetic background, the course of infection was intermediate between the 2 parental lines, suggesting that although *Py*EBL is a critical determinant, other factor(s) are also involved in the lethal phenotype of the 17XL line. In *P. falciparum*, the expression of EBL seems to be co-operationally regulated with another *Plasmodium* ligand encoded by the *rbl (reticulocyte-binding-like)* multigene family that is composed of 6 members in *P. falciparum* and at least 14 members in *P. yoelii* (14–16); thus, the *P. yoelii rbl* protein, Py235, is a potential candidate for such factor(s). Consistent with this hypothesis is the finding that when Py235 expression was suppressed, the course of infection of the lethal *P. yoelii* YM line was altered from a lethal pattern to an intermediate pattern similar to that observed in the 17X-CtoR line shown in this study (17). On the basis of these observations, we propose that *Py*EBL may preferentially recognize reticulocytes and that the removal of *Py*EBL from the micronemes may result in free space within this organelle that may subsequently be filled with other ligand(s), possibly Py235, which consequently enables the parasite to invade a variety of erythrocyte types. Because different Py235 proteins may have different receptor specificities, parasite invasion preference and the subsequent course of infection may vary, depending on the Py235 member that fills the free space in the micronemes created by the absence of *Py*EBL. Such a switching mechanism for an erythrocyte invasion pathway has been previously proposed for *P. falciparum* (18).

A Linkage Group Selection analysis conducted by Pattaradilokrat et al. (19) identified a chromosomal region that included the *ebl* gene locus as a major determinant in the multiplication rate differences between the lethal *P. y. yoelii* YM line and a nonlethal 33X line, supporting the role of the EBL protein in controlling virulence phenotypes. Consistent with our findings that another genetic factor may be involved, they also identified a further genomic region on *P. yoelii* chromosome 5 or 6 that showed weak association with multiplication rate.

Because *Py*EBL localized in the dense granules is potentially nonfunctional, we attempted to disrupt the *pyebl* gene locus in both the 17X and 17XL lines (Fig. S7). However, repeated attempts failed to achieve this, despite the successful genomic integration of the control plasmid. This indicates that *Py*EBL is essential for parasite survival, even when it is not trafficked to the microneme. Two possible explanations for this may be that (*i*) an undetectable amount of *Py*EBL may still localize in the micronemes and remain functional, or (*ii*) *Py*EBL is functional during erythrocyte invasion (or for another unknown critical role during the life cycle), even when localized in the dense granules. Although a subgroup of the dense granules, known as exonemes, were recently reported to secrete their contents immediately before schizont rupture (20), we found that *Py*EBL was not detected on the surface of released individual merozoites of 17XL parasites (Fig. S8). Thus, the identity of the *Py*EBL-containing dense granules and the timing of *Py*EBL secretion from them, if at all, in the 17XL line remain undetermined.

In summary, we have found that a single nucleotide substitution altered the intracellular localization of the malaria parasite ligand *Py*EBL, which in turn altered erythrocyte invasion preference, course of infection, and parasite virulence. The virulence-mediating mechanism described in this report furthers our understanding of parasite–host interactions and has important implications for malaria vaccine design, especially those based on *Pv*DBP for *P. vivax* malaria.

Materials and Methods

Rodent Malaria Parasites. *Plasmodium yoelii* 17X, 17XL, and YM lines were maintained in BALB/c mice (Charles River Japan). The *P. yoelii* YM line was a kind gift from David Walliker of Edinburgh University.

DNA and RNA Isolation. Parasite genomic DNA (gDNA) was isolated from parasite-infected mouse blood using DNAzol BD reagent (Invitrogen). Parasite-infected blood was passed through a single CF11 cellulose column to remove leukocytes, and a schizont-enriched fraction was collected by differential centrifugation on a 50% Percoll solution (GE Healthcare). Total RNA was isolated from the schizont-enriched fraction using RNeasy Mini Kit (Qiagen). cDNA was synthesized using Omniscript reverse transcriptase (Qiagen) with random hexamer after DNase treatment.

PCR Amplification and Sequencing of *ebl* Genes. *ebl* genes were PCR-amplified from gDNA using KOD Plus DNA polymerase (Toyobo), with specific primers for each *ebl* gene designed using the *P. yoelii* genome database (The Institute for Genomic Research) and the *P. chabaudi* and *P. berghei* genome databases (The Sanger Centre). *ebl* sequences were determined by direct sequencing using an ABI PRISM 310 genetic analyzer (Applied Biosystems) from PCR-amplified products. Sequences were aligned using CLUSTALW implemented in MacVector (version 9.0; Accelrys).

Southern Blot Analysis. Five micrograms of *P. yoelii* gDNA were digested with EcoRI, EcoRV, ClaI, BanI, and NspI, and with BanI and HpaI with appropriate buffer, overnight. Digested gDNA was subjected to electrophoresis on 0.8% agarose gels, followed by alkaline transfer onto a Hybond-*n* + PVDF membrane (GE Healthcare). Probes were first PCR-amplified with 5′–TAAATCTAAATGGGATACAT–3′ and 5′–AGTTGGATTGATAGTTACAGATTC–3′ primers for the *pyebl* region, cloned into pGEM-T Easy plasmid (Promega), digested from the plasmid, and then hybridized onto membranes. Probes were labeled with the AlkPhos Direct kit (GE Healthcare), and a chemiluminescent signal developed with CDP-*star* reagent (GE Healthcare) was recorded on RX-U film (Fujifilm).

Recombinant Proteins. Expression plasmids were constructed on the basis of the pEU-E01-G(TEV)-N2 vector (21) by inserting PCR products amplified from *P. yoelii* 17X gDNA using KOD Plus DNA polymerase with the following primers: 5′-gagaCTCGAGGTTAATTTATTAAAAAGAACATATGAATCTTTCC-3′ and 5′-tctcGGATCC**CTA**TGAATAGCTCTCTTTTTGAAAAC-3′ for *Py*EBL regions 1 to 6 (R1–6; amino acid positions 28–787), 5′-gagaCTCGAGGTTAATTTATTAAAAAGAACATATGAATCTTTCC-3′ and 5′-tctcGGATCC**CTA**CAAATTATTATTAATAGGAGTATTACTGGG-3′ for regions 1 to 2 (R1–2; 28–436), 5′-gagaCTCGAGGAAAAAAATGGAAATGTAAATTACAAAG-3′ and 5′-tctcGGATCC**CTA**CAAATTATTATTAATAGGAGTATTACTGGG-3′ for region 2 (R2; 113–436), 5′-gagaCTCGAGTCTTCTGTTAAACCCAGTAATAC-3′ and 5′-tctcGGATCC**CTA**TACATTTTCGTTGGCTAGC-3′ for regions 3 to 5 (R3–5; 423–716), and 5′-gagagagaCTCGAGGACCCTAAACATGTATGTGTTGATAC-3′ and 5′-gagagagaGGATCC**TCA**TCCCATAAAGCTGGAAGAACTACAG-3′ for the 19-kDa region of the merozoite surface protein 1, *Py*MSP1 (*Py*MSP1–19; 1658–1757). The stop codon is shown in bold letters, and XhoI and BamHI restriction sites are underlined. GST-fused *Py*EBL or *Py*MSP1–19 recombinant proteins were expressed using the wheat germ cell-free protein synthesis system (Protemist DT; CellFree Sciences). Recombinant proteins were captured by a glutathione

column, washed, and eluted with glutathione elution buffer. Protein synthesis was confirmed by SDS-PAGE and Coomassie Brilliant Blue protein staining. Recombinant *Py*EBL R1–6 and R3–5 and *Py*MSP1–19 were used to produce antibodies, and *Py*EBL R1–2 and R2 were used for Western blot analysis.

Antibodies. To produce mouse anti-*Py*EBL and anti-*Py*MSP1 sera, female BALB/c mice were i.p. immunized 5 times with recombinant *Py*EBL R1–6 or 3 times with recombinant *Py*MSP1–19 emulsified with Freund's adjuvant, and killed for serum collection. To produce rabbit anti-*Py*EBL R3–5 serum, a female Japanese white rabbit was s.c. immunized 3 times with recombinant *Py*EBL R3–5 emulsified with Freund's adjuvant. To produce mouse anti-*Py*EBL monoclonal antibodies, the spleen was removed from a mouse immunized with recombinant *Py*EBL R1–6, and spleen cells were fused with a mouse myeloma cell line derived from a BALB/c mouse by the conventional polyethylene glycol method. Supernatants of cultured hybridoma colonies were tested with recombinant *Py*EBL R1–6 by ELISA and on *P. yoelii* 17X blood smears by indirect immunofluorescent assay. Positive hybridoma colonies were selected and cloned by 2 rounds of limiting dilution. The epitope region of each monoclonal antibody was tested by Western blot with a panel of recombinant *Py*EBL proteins. Anti-AMA1 rabbit serum was a gift from Carole Long of the National Institutes of Health.

Immunofluorescence Microscopy. *P. yoelii*–infected mouse erythrocytes were smeared onto glass slides, air dried, and stored at −80 °C without fixation. Slides were thawed, acetone-fixed, preincubated with PBS containing 5% nonfat milk at 37 °C for 30 min, incubated with mouse anti-*Py*EBL and rabbit anti-AMA1 sera at room temperature for 1 h, and then incubated with FITC-conjugated goat anti-(mouse IgG and IgM) antibody (Biosource International) and Alexa-546–conjugated goat antirabbit IgG antibody (Molecular Probes) at 37 °C for 30 min. Parasite nuclei were stained with DAPI. Differential interference contrast (DIC) and fluorescent images were obtained using a fluorescence microscope (BX50; Olympus) with a CCD digital camera (DC500; Leica) and processed using Adobe Photoshop CS (version 8.0; Adobe Systems).

Immunoelectron Microscopy. *P. yoelii*–infected mouse blood was fixed in 1% paraformaldehyde–0.1% glutaraldehyde in Hepes-buffered saline and embedded in LR white resin (Polysciences). Sections were blocked for 30 min in PBS–milk–Tween 20, incubated overnight at 4 °C in PBS–milk–Tween 20 containing mouse anti-*Py*EBL R1–6 serum, and then incubated for 1 h in PBS–milk–Tween 20 containing goat antimouse IgG conjugated with gold particles (10 nm diameter; Jansen). Sections were stained with 2% uranyl acetate in 50% methanol and examined by electron microscopy (JEM-1230; JEOL).

Genetic Modification of the *pyebl* Gene Locus. Two basic plasmids, pPbDT3U-B12 and pHDEF1-mh-R12, were constructed. A DNA fragment encoding cyan fluorescent protein was PCR-amplified from pECFP-C1 plasmid (Stratagene) using KOD Plus DNA polymerase with primers 5′-agcGCTAGCGTGAGCAAGGGCGAG-3′ (NheI site is underlined) and 5′-gacGTCGAC**GGATCC**TCTAGACTTGTACAGCTCGTCC-3′ (SalI and XbaI sites are underlined, and BamHI site is shown in bold) and ligated into the pGEM-T Easy plasmid. The insert was then digested with NheI and SalI, purified, and ligated into pRGDT-B12 (22) using the NheI and SalI sites, yielding pRCDT-B12. pRCDT-B12 was digested with ClaI and XbaI and filled with an oligonucleotide linker comprising cgatCTCGAG**CCCGGG**t and ctaga**CCCGGG**CTCGAGat to generate XhoI (underlined) and SmaI (bold) sites to yield pPbDT3U-B12. pHDEF1-mh (23) was digested with SmaI and ApaI to remove the 3′ untranslated region of histidine-rich protein 2, the ApaI cohesive end was blunted, and a Gateway gene conversion cassette C1 (Invitrogen) was inserted. The XhoI site was destroyed by XhoI digestion, filled in using KOD Plus DNA polymerase, and self-ligated to yield pHDEF1-mh-R12.

To modify the *pyebl* gene locus, a DNA fragment encoding *Py*EBL region 6 to the stop codon was PCR-amplified from gDNA of the *P. yoelii* 17XL line with primers 5′-gCCATGGGAACATAGAGACATTAAAAAAAGC-3′ and 5′-gCTCGAGATAAAAATCTACAGGTATATATTC-3′ (NcoI and XhoI sites are underlined) and cloned into pGEM-T Easy plasmids. The insert was ligated into the NcoI and XhoI sites of pPbDT3U-B12 to yield pR6Cyt-B12. DNA fragments encoding *Py*EBL region 3 to the stop codon were PCR-amplified from cDNA of the *P. yoelii* 17X and 17XL lines with primers 5′-atCTTCTGTTAAACCCAGTAATAC-3′ and 5′-ccAGATCTTTAATAAAAATCTACAGGTATATATTC-3′ (BglII site is underlined). PCR products were then ligated into the SmaI site of pR6Cyt-B12, yielding pR6Cyt+R3Cyt(X)-B12 and pR6Cyt+R3Cyt(XL)-B12, respectively. pR6Cyt+R3Cyt(X)-B12 and pR6Cyt+R3Cyt(XL)-B12 were subjected to a BP recombination reaction with the donor vector pDONR221 (Invitrogen) to produce the corresponding entry plasmids pENT.R6Cyt+R3Cyt(X) and pENT.R6Cyt+R3Cyt(XL). These entry plasmids were subjected to a LR recombination reaction (Invitrogen), according to the manufacturer's instructions, with pHDEF-1-mh-R12 to yield replacement constructs pYEBL-R6Cyt+R3Cyt(X) and pYEBL-R6Cyt+R3Cyt(XL), respectively.

P. yoelii schizont-enriched fraction was collected by differential centrifugation on 50% HistoDenz in PBS, and 20 μg of XhoI-digested transfection constructs were electroporated to 5×10^7 of enriched schizonts using the Nucleofector device (Amaxa) with human T cell solution under program U-33 (24). Transfected parasites were i.v. injected into 8-week-old BALB/c female mice, which were treated by i.p. injection with 1 mg/kg of pyrimethamine daily. Before inoculation of 17X line parasites, mice were treated with phenylhydrazine to increase the reticulocyte population in the blood. Drug-resistant parasites were cloned by limiting dilution. Integration of the transfection constructs was confirmed by PCR amplification with a unique set of primers for the modified *pyebl* gene locus, followed by sequencing and Southern blot analysis.

Course of Infection. To assess the course of infection of transgenic and WT parasite lines, 1×10^6 parasitized erythrocytes were injected i.v. into 8-week-old female BALB/c mice. Thin blood smears were made daily, stained with Giemsa's solution, and parasitemias were recorded. Mouse survival was evaluated by the Kaplan-Meier method. Parasitemias of each group were compared by 1-way ANOVA and Tukey's posttest, implemented in Prism 4.0 (GraphPad Software).

Selectivity Index. To compare erythrocyte preference between transgenic and WT *P. yoelii* parasite lines, a SI was calculated as follows: Multiple-infected erythrocytes divided by the expected number of multiple-infected erythrocytes, which was calculated from the number of infected erythrocytes and parasitemia (13). When the preferred erythrocyte type is limited, the observed number of multiple-infected erythrocytes increases. More than 200 parasitized erythrocytes were examined on Giemsa-stained thin blood smears collected on postinoculation day 3. The SI of each group was compared by 1-way ANOVA and Tukey's posttest, implemented in Prism 4.0.

For additional information see *SI Materials and Methods.*

ACKNOWLEDGMENTS. We thank D. Walliker for *P. yoelii* 33X, 33XPr3, and YM lines; C. Long for anti-AMA1 rabbit serum; H. A. del Portillo (Barcelona Centre for International Health Research, Barcelona) for pHDEF1-mh; Y. Tanaka, K. Kameda, and K. Oka (Integrated Center for Science, Ehime University) for their expertise; N. Kangwanrangsan (Ehime University, Matsuyama, Japan) for anti-*Py*MSP1–19 serum; and R. Culleton for critical reading. Preliminary sequence data for *P. berghei*, *P. chabaudi*, and *P. vinckei* were obtained from The Institute for Genomic Research. Animal experiments were carried out in compliance with the Guide for Animal Experimentation at Ehime University School of Medicine. This work was supported in part by Grants-in-Aids for Scientific Research 19790308 (to H.O.), 19590428 (to O.K.), 16390126 and 19390120 (to M. Torii), by Scientific Research on Priority Areas 19041053 (to T.T.) from the Ministry of Education, Culture, Sports, Science and Technology of Japan, and by Japan Society for the Promotion of Science–National University of Singapore Joint Research Program 07039011–000161 (to O.K.).

1. Landau I, Gautret P (1998), in *Malaria: Parasite Biology, Pathogenesis, and Protection*, ed Sherman IW (American Society for Microbiology, Washington, DC), pp 401–417.
2. Yoeli M, Hargreaves B, Carter R, Walliker D (1975) Sudden increase in virulence in a strain of *Plasmodium berghei yoelii*. *Ann Trop Med Parasitol* 69:173–178.
3. Playfair JH, De Souza JB, Cottrell BJ (1977) Protection of mice against malaria by a killed vaccine: Differences in effectiveness against *P. yoelii* and *P. berghei*. *Immunology* 33:507–515.
4. Miller LH, Mason SJ, Clyde DF, McGinniss MH (1976) The resistance factor to *Plasmodium vivax* in blacks. The Duffy-blood-group genotype, FyFy. *N Engl J Med* 295:302–304.
5. Wertheimer SP, Barnwell JW (1989) Plasmodium vivax interaction with the human Duffy blood group glycoprotein: Identification of a parasite receptor-like protein. *Exp Parasitol* 69:340–350.
6. Greenwood BM, et al. (2008) Malaria: Progress, perils, and prospects for eradication. *J Clin Invest* 118:1266–1276.
7. Adams JH, et al. (1992) A family of erythrocyte binding proteins of malaria parasites. *Proc Natl Acad Sci USA* 89:7085–7089.
8. Withers-Martinez C, et al. (2008) Malarial EBA-175 region VI crystallographic structure reveals a KIX-like binding interface. *J Mol Biol* 375:773–781.
9. Treeck M, et al. (2006) A conserved region in the EBL proteins is implicated in microneme targeting of the malaria parasite *Plasmodium falciparum*. *J Biol Chem* 281:31995–32003.

10. Sim BK, Toyoshima T, Haynes JD, Aikawa M (1992) Localization of the 175-kilodalton erythrocyte binding antigen in micronemes of *Plasmodium falciparum* merozoites. *Mol Biochem Parasitol* 51:157–159.
11. Adams JH, et al. (1990) The Duffy receptor family of *Plasmodium knowlesi* is located within the micronemes of invasive malaria merozoites. *Cell* 63:141–153.
12. Torii M, Adams JH, Miller LH, Aikawa M (1989) Release of merozoite dense granules during erythrocyte invasion by *Plasmodium knowlesi*. *Infect Immun* 57:3230–3233.
13. Simpson JA, Silamut K, Chotivanich K, Pukrittayakamee S, White NJ (1999) Red cell selectivity in malaria: A study of multiple-infected erythrocytes. *Trans R Soc Trop Med Hyg* 93:165–168.
14. Stubbs J, et al. (2005) Molecular mechanism for switching of *P. falciparum* invasion pathways into human erythrocytes. *Science* 309:1384–1387.
15. Iyer J, Grüner AC, Rénia L, Snounou G, Preiser PR (2007) Invasion of host cells by malaria parasites: A tale of two protein families. *Mol Microbiol* 65:231–249.
16. Carlton JM, et al. (2002) Genome sequence and comparative analysis of the model rodent malaria parasite *Plasmodium yoelii yoelii*. *Nature* 419:512–519.
17. Iyer JK, Amaladoss A, Ganesan S, Preiser PR (2007) Variable expression of the 235 kDa rhoptry protein of *Plasmodium yoelii* mediate host cell adaptation and immune evasion. *Mol Microbiol* 65:333–346.
18. Duraisingh MT, Maier AG, Triglia T, Cowman AF (2003) Erythrocyte-binding antigen 175 mediates invasion in *Plasmodium falciparum* utilizing sialic acid-dependent and -independent pathways. *Proc Natl Acad Sci USA* 100:4796–4801.
19. Pattaradilokrat S, Culleton RL, Cheesman SJ, Carter R (2009) Gene encoding erythrocyte binding ligand linked to blood stage multiplication rate phenotype in *Plasmodium yoelii yoelii*. *Proc Natl Acad Sci USA*, 10.1073/pnas.0811430106.
20. Yeoh S, et al. (2007) Subcellular discharge of a serine protease mediates release of invasive malaria parasites from host erythrocytes. *Cell* 131:1072–1083.
21. Tsuboi T, et al. (2008) Wheat germ cell-free system-based production of malaria proteins for discovery of novel vaccine candidates. *Infect Immun* 76:1702–1708.
22. Ghoneim A, Kaneko O, Tsuboi T, Torii M (2007) The *Plasmodium falciparum* RhopH2 promoter and first 24 amino acids are sufficient to target proteins to the rhoptries. *Parasitol Int* 56:31–43.
23. Fernandez-Becerra C, de Azevedo MF, Yamamoto MM, del Portillo HA (2003) Plasmodium falciparum: New vector with bi-directional promoter activity to stably express transgenes. *Exp Parasitol* 103:88–91.
24. Janse CJ, et al. (2006) High efficiency transfection of *Plasmodium berghei* facilitates novel selection procedures. *Mol Biochem Parasitol* 145:60–70.

INFECTION AND IMMUNITY, Dec. 2009, p. 5496–5500
0019-9567/09/$12.00 doi:10.1128/IAI.00640-09

Vol. 77, No. 12

Malaria Ookinete Surface Protein-Based Vaccination via the Intranasal Route Completely Blocks Parasite Transmission in both Passive and Active Vaccination Regimens in a Rodent Model of Malaria Infection▽

Takeshi Arakawa,[1,2] Mayumi Tachibana,[3] Takeshi Miyata,[1] Tetsuya Harakuni,[1] Hideyasu Kohama,[1] Yasunobu Matsumoto,[4] Naotoshi Tsuji,[5] Hajime Hisaeda,[6]† Anthony Stowers,[6]‡ Motomi Torii,[3] and Takafumi Tsuboi[7]*

Molecular Microbiology Group, COMB, Tropical Biosphere Research Center, University of the Ryukyus, 1 Senbaru, Nishihara, Okinawa 903-0213, Japan[1]; Division of Host Defense and Vaccinology, Graduate School of Medicine, University of the Ryukyus, 207 Uehara, Nishihara, Okinawa 903-0215, Japan[2]; Department of Molecular Parasitology, Ehime University School of Medicine, Shigenobu-cho, Ehime 791-0295, Japan[3]; Laboratory of Global Animal Resource Science, Department of Global Agricultural Sciences, Graduate School of Agricultural and Life Sciences, University of Tokyo, 1-1-1 Yayoi, Bunkyo-ku, Tokyo 113-8657, Japan[4]; National Institute of Animal Health, National Agricultural Research Organization, 3-1-5 Kannondai, Tsukuba, Ibaraki 305-0856, Japan[5]; Malaria Vaccine Development Unit, National Institute of Allergy and Infectious Diseases, National Institutes of Health, Rockville, Maryland[6]; and Cell-Free Science and Technology Research Center, Ehime University, Matsuyama, Ehime 790-8577, Japan[7]

Received 5 June 2009/Returned for modification 6 July 2009/Accepted 6 September 2009

Malaria vaccines based on ookinete surface proteins (OSPs) of the malaria parasites block oocyst development in feeding mosquitoes and hence disrupt the parasite life cycle and prevent the disease from being transmitted to other individuals. To investigate whether a noninvasive mucosal vaccination regimen effectively blocks parasite transmission in vivo, *Plasmodium yoelii* Pys25, a homolog of the Pfs25 and Pvs25 OSPs of *Plasmodium falciparum* and *Plasmodium vivax*, respectively, was intranasally (i.n.) administered using a complement-deficient DBA/2 mouse malaria infection model, in which a highly elevated level of oocysts develops in feeding mosquitoes. Vaccinated mice developed a robust antibody response when the vaccine antigen was given together with cholera toxin adjuvant. The induced immune serum was passively transferred to DBA/2 mice 3 days after infection with *P. yoelii* 17XL, and *Anopheles stephensi* mosquitoes were allowed to feed on the infected mice before or after serum transfusion. This passive immunization completely blocked oocyst development; however, immune serum induced by the antigen or adjuvant alone did not have such a profound antiparasite effect. Further, when i.n. vaccinated mice were infected with the parasite and then mosquitoes were allowed to directly feed on the infected mice, complete blockage of transmission was again observed. To our knowledge, this is the first time that mucosal vaccination has been demonstrated to be efficacious for directly preventing parasite transmission from vaccinated animals to mosquitoes, and the results may provide important insight into rational design of nonparenteral vaccines for use against human malaria.

Malaria is one of the most important infectious diseases, and the levels of mortality and morbidity are high, especially among children in developing countries in Africa, Asia, and South America. Implementation of malaria control measures, such as antimalaria drug chemotherapy and insecticide-treated bed nets, has made a significant contribution to reducing the incidence of malaria in many parts of the world. However, these control measures may not be sufficient, and therefore new tools, including vaccines, should be included in a new malaria control campaign for local elimination and final eradiation of malaria from the globe (7). A promising strategy to counteract global malaria endemicity is to develop highly efficacious vaccines, and several promising candidates have been intensively investigated (7, 20); vaccines targeting asexual stages (i.e., sporozoite, hepatic, and erythrocytic stages) are designed to prevent infection and reduce disease severity, while vaccines that target the sexual stage, in which the parasite undergoes sporogonic development in anopheline mosquitoes, prevent vector-mediated transmission of the parasite from person to person (4, 8, 14, 17, 25). Although transmission-blocking vaccines do not directly prevent infection, they reduce parasite infectivity for the vector and consequently lower the mosquito infection rate and the frequency of transmission to humans. In addition, this strategy is believed to be particularly useful for controlling escape of mutants from vaccines designed based on antigens expressed at an asexual stage; therefore, transmission-blocking vaccines are increasingly being considered indispensable components of malaria vaccine strategies and are key components of malaria elimination (10, 11).

* Corresponding author. Mailing address: Cell-Free Science and Technology Research Center, Ehime University, 3 Bunkyo-cho, Matsuyama, Ehime 790-8577, Japan. Phone: 81-89-927-8277. Fax: 81-89-927-9941. E-mail: tsuboi@ccr.ehime-u.ac.jp.

† Present address: Department of Immunology and Parasitology, Faculty of Medical Sciences, Kyushu University, Fukuoka, Fukuoka 812-8582, Japan.

‡ Present address: CSL Limited A.C.N. 051 588 348, 45 Poplar Road, Parkville, Victoria 3052, Australia.

▽ Published ahead of print on 14 September 2009.

Studies on rodent and human malaria concluded that an effector mechanism that is pivotal for blocking transmission is induction of antigen-specific serum antibodies in a vaccinated host, from which female mosquitoes, when they bite to obtain blood meal, coingest gametocyte pairs together with the induced antibodies (2, 3, 5, 9, 18, 24). The ingested antibodies seem to be stable in the mosquito midgut, at least in the time frame within which the transmitted gametocytes develop into ookinetes.

Parasite antigens expressed later at the postfertilization stage in the mosquito midgut, such as ookinete surface proteins (OSPs), including Pfs25 and Pvs25 from *Plasmodium falciparum* and *Plasmodium vivax*, respectively, are particularly important vaccine targets because they are likely to be concealed immunologically, if not concealed completely, from the mammalian host's immunosurveillance system, which suggests that there is a reduced driving force to produce the antigenic variations often observed for antigens expressed at prefertilization stages (6, 12, 23, 28). In addition, several recent studies indicated that in the malaria life cycle the ookinete-to-oocyst transition stage is one of the most vulnerable stages of parasite development, making the postfertilization stage of sporogonic development an ideal target for antitransmission vaccines.

The vast majority of pathogens invade through mucosal tissues and therefore can be controlled effectively by mucosal vaccines rather than parenteral vaccines. Notwithstanding the great merit of mucosal vaccines, most vaccines in use today are delivered parenterally (subcutaneously [s.c.] or intramuscularly). In spite of many arguments against the concept that vaccines against arthropod vector-borne human pathogens, such as malaria parasites, could be designed based on mucosal delivery, recent studies performed by us and other workers demonstrated that mucosal vaccines could be efficacious for prevention of arthropod-transmitted infections, because mucosal administration of foreign antigens mixed with a potent mucosal adjuvant, such as cholera toxin (CT), can induce strong systemic immunity (2, 3, 13). Here we extended our previous studies to test our hypothesis that the malaria OSPs are sufficiently immunogenic when they are administered by the intranasal (i.n.) route in the presence of a mucosal adjuvant, which should in theory effectively block parasite transmission to feeding mosquitoes when both passive and active vaccination regimens are used.

MATERIALS AND METHODS

Mice, vaccination, and antibody enzyme-linked immunosorbent assay (ELISA). Seven-week-old female DBA/2NCrj (DBA/2) mice were purchased from Japan SLC (Tokyo, Japan). Complement C5-deficient DBA/2 mice were used for live mosquito-feeding experiments, because the highly elevated levels of oocysts that developed in the mosquito midgut were useful for evaluation of transmission-blocking vaccine efficacy (26).

Mice were i.n. vaccinated once a week for 4 weeks with 25 μg of yeast-derived recombinant *Plasmodium yoelii* Pys25 synthesized and purified like Pvs25 as described previously (14) in the absence or presence of 1 μg of CT (Sigma-Aldrich). As a control, a group of mice were vaccinated with 1 μg of CT alone. For passive vaccination experiments, DBA/2 mice were intravenously vaccinated with 0.5 ml of pooled immune sera derived from mice vaccinated i.n. with Pys25 plus CT, with Pys25 alone, or with CT alone.

For ELISA of vaccine-induced immune sera, a flat-bottom 96-well microtiter plate (Immulon 4; Dynex Technology Inc., Chantilly, VA) was coated with recombinant Pys25 (0.5 μg/well in bicarbonate buffer, pH 9.6) and blocked with 1% skim milk in Tris-buffered saline containing 0.05% Tween 20. Immune sera serially diluted with the blocking buffer were applied to wells in duplicate (100 μl/well) and incubated for 2 h at 37°C, which was followed by addition of alkaline phosphatase-conjugated anti-mouse antibody for immunoglobulin (Ig) isotype and IgG subclass analysis. The alkaline phosphatase substrate (*p*-nitrophenyl phosphate [Sigma-Aldrich]) was added, and the absorbance at 490 nm was determined with a microplate reader (Bio-Rad Laboratories). The antibody concentration was determined based on known amounts of mouse Igs used as a standard. The statistical significance of differences in antibody concentration or absorbance was determined by Student's *t* test.

Parasite infection, blood feeding experiment, and assay of transmission blocking. For analysis of the parasite-killing effect of i.n. vaccination-induced immune sera, mice were intraperitoneally inoculated with 10^6 peripheral red blood cells that had been infected with *P. yoelii* strain 17XL, and the infected mice were maintained for 3 days until the level of parasitemia reached 9 to 10%, which was determined by microscopic examination of Giemsa-stained thin blood smear preparations. Then approximately 100 *Anopheles stephensi* mosquitoes that had been starved overnight were allowed to obtain a blood meal from the infected mice either before or 1 h after intravenous injection of immune sera that had been prepared from mice 1 week after the last i.n. vaccination with Pys25 plus CT, with Pys25 alone, or with CT alone. Fully engorged mosquitoes were maintained at 24°C for 1 week by giving them water containing 1.5% fructose and 1.5% sucrose. For each experimental group, mosquitoes were dissected, and their midguts were examined with a light microscope to count the number of oocysts.

For analysis of the direct parasite transmission-blocking efficacy of i.n. vaccination, mice vaccinated with Pys25 plus CT, with Pys25 alone, or with CT alone were infected as described above with the parasite 1 week after the last vaccination, and then mosquitoes were allowed to feed directly on the infected animals; this was followed by enumeration of the oocysts that developed.

The statistical significance of differences in the numbers of oocysts was determined by the Kruskal-Wallis test or the Wilcoxon-Mann-Whitney U test by using the software JMP (SAS Institute Inc.).

RESULTS

A significant level of specific serum IgG and IgM antibodies (mainly IgG) was induced in DBA/2 mice by i.n. vaccination with Pys25 plus CT (14,147 ± 4,241 μg/ml) but not by i.n. vaccination with Pys25 alone or CT alone (Fig. 1a, upper panel). Oral inoculation of 50 μg of Pys25, however, did not induce an antibody response even in the presence of 10 μg CT (data not shown). IgG1 was found to be the predominant serum IgG subclass, and almost no IgG2a was detected in mice vaccinated with Pys25 plus CT, an indication of the Th2 type of immune response induction (Fig. 1a, lower panel). Low but detectable levels of Pys25-specific serum IgA and IgE were seen in the group vaccinated with Pys25 plus CT but not in the group vaccinated with Pys25 alone or CT alone (Fig. 1b). Similar humoral immune responses were observed when outbred ddy mice were used for the immunization experiments (data not shown).

To evaluate the parasite transmission-blocking effect of the induced immune sera in vivo, *A. stephensi* mosquitoes were allowed to obtain a blood meal from DBA/2 mice that had been infected with *P. yoelii* 17XL before or after passive transfer of the immune sera of mice vaccinated i.n. with Pys25 plus CT, with Pys25 alone, or with CT alone as described in Materials and Methods. For all three immunization groups, large numbers of oocysts were observed in the mosquito midgut when the mosquitoes were allowed to feed before the immune sera were transferred (median for CT alone, 346 oocysts; median for Pys25 alone, 302 oocysts; median for Pys25 plus CT, 311 oocysts) (Fig. 2a). In contrast, when the mosquitoes received the blood meal after the immune sera were transferred, oocyst formation was completely blocked in the group vaccinated with Pys25 plus CT, but not in the group vaccinated with

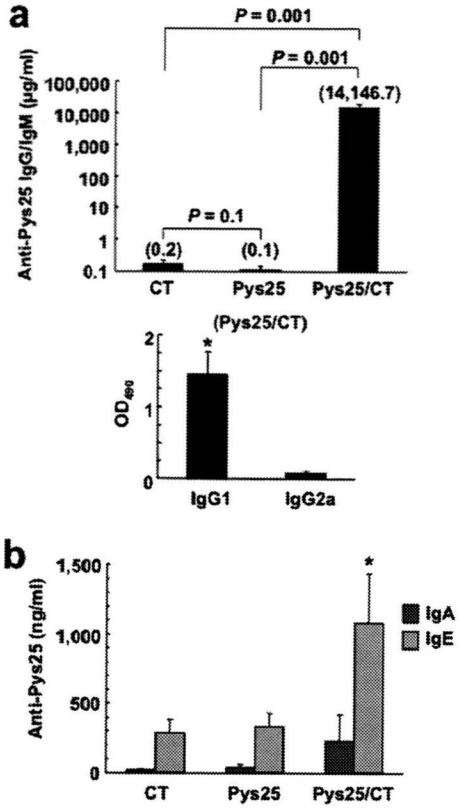

FIG. 1. Antibody responses in mice i.n. vaccinated with recombinant Pys25. DBA/2 mice (three or four mice/group) were vaccinated i.n. with a mixture of Pys25 (25 μg) and CT (1 μg), with Pys25 alone (25 μg), or with CT alone (1 μg) once a week for 4 weeks, and 1 week after the final vaccination serum antibody titers were analyzed by ELISA. (a) (Upper panel) Pys25-specific serum IgG and IgM (predominantly IgG) levels expressed as mean antibody concentrations in the serum. The error bars indicate standard deviations. (Lower panel) Immune sera (1/128,000) from mice vaccinated with Pys25 plus CT were also analyzed for the presence of IgG1 and IgG2a, and the results were expressed as mean optical densities at 490 nm (OD_{490}). The error bars indicate standard deviations. *, $P = 0.002$ for comparison of IgG1 and IgG2a. (b) Pys25-specific serum IgA and IgE levels expressed as mean antibody concentrations in serum (ng/ml). The error bars indicate standard deviations. *, $P < 0.01$ for a comparison of Pys25 plus CT and CT or Pys25. No significant differences between groups were observed for serum IgA. Statistical significance was determined by Student's *t* test.

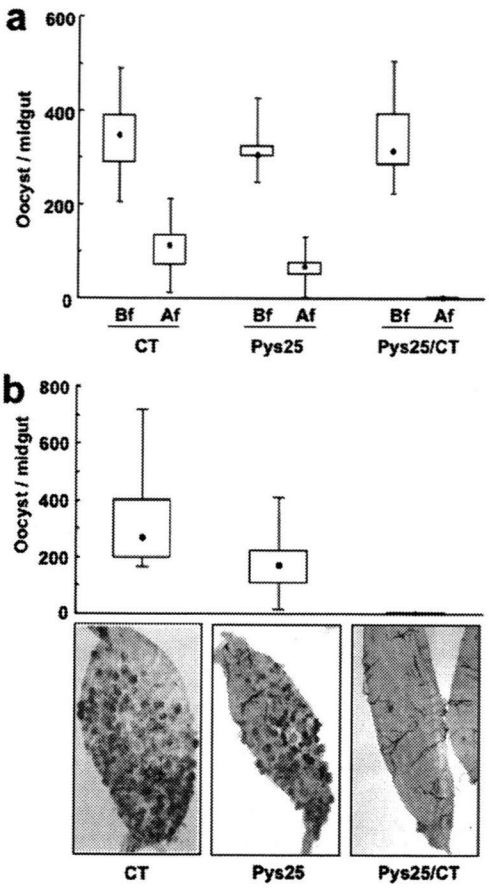

FIG. 2. Transmission-blocking vaccine efficacy. (a) Transmission-blocking effects of passively transferred immune sera on *P. yoelii* oocyst development in the *A. stephensi* mosquito midgut. Approximately 100 mosquitoes were allowed to feed on parasite-infected mice (9 to 10% parasitemia at the time of feeding) before (Bf) or after (Af) intravenous injection of immune sera derived from mice i.n. vaccinated with Pys25 plus CT, with Pys25 alone, or with CT alone. Data are expressed as the median numbers of oocysts per mosquito (dots in boxes), quartiles (boxes), and ranges (lines above and below boxes). Statistically significant differences were found in all three immunization groups compared for the treatment after intravenous injection of immune sera ($P < 0.0001$) but not for the treatment before intravenous injection of immune sera ($P = 0.726$) in an analysis performed using the Kruskal-Wallis test. There are also statistically significant differences between the treatment before intravenous injection of immune sera and the treatment after intravenous injection of immune sera for all three immunization groups ($P < 0.0001$, Wilcoxon-Mann-Whitney U test). (b) Transmission-blocking effects of active immunization on oocyst development. Mice were i.n. vaccinated with Pys25 plus CT, with Pys25 alone, or with CT alone and then were infected with the parasite. Mosquitoes were allowed to directly feed on infected mice, the numbers of oocysts were determined, and the data were expressed as described above for panel a. Statistically significant differences were found in all three groups compared by using the Kruskal-Wallis test ($P < 0.0001$). Light microscopic images of representative mosquito midguts from the active vaccination experiments are shown at the bottom.

CT alone (median, 109 oocysts) or with Pys25 alone (median, 65 oocysts). Although we do not know why the CT or Pys25 immune serum had a significant parasite-killing effect (for CT, 346 oocysts versus 109 oocysts; for Pys25, 302 oocysts versus 65 oocysts), no mosquitoes completely lacked oocysts when they were given CT or Pys25 immune serum (Table 1). The results demonstrated that i.n. vaccination with Pys25 plus CT induced antibodies which confer complete transmission-blocking immunity when a passive vaccination regimen is used.

Next, to evaluate the direct mucosal vaccine efficacy of Pys25, mosquitoes were allowed to obtain a blood meal directly from parasite-infected mice that had been vaccinated as described in Materials and Methods. The results demonstrated that vaccination with Pys25 plus CT completely blocked oocyst development, as we observed in the passive vaccination experiment, while significant numbers of oocysts were observed in mosquitoes that fed on CT-vaccinated mice (median, 269 oo-

TABLE 1. Prevalence of oocyst infection in *A. stephensi* mosquitoes

Type of immunization	Vaccine	No. of oocyst-positive mosquitoes/ total no. examined (% infection)[a]	No. of oocyst-positive mosquitoes/total no. examined (% infection)[a]	
			Before immune serum transfer[b]	After immune serum transfer[b]
Passive	CT		31/31 (100)	40/40 (100)
	Pys25		71/71 (100)	39/39 (100)
	Pys25 + CT		51/51 (100)	0/56 (0)
Active	CT	150/150 (100)		
	Pys25	90/90 (100)		
	Pys25 + CT	0/84 (0)		

[a] The percentages are the percentages of oocyst-positive mosquitoes based on the total numbers of mosquitoes examined.

[b] Approximately 100 mosquitoes were allowed to feed on parasite-infected mice (9 to 10% parasitemia at the time of feeding) before or after intravenous transfer of immune sera obtained from mice i.n. vaccinated with Psy25 plus CT, with Psy25 alone, or with CT alone.

cysts) or Pys25-vaccinated mice (median, 170.5 oocysts) (Fig. 2b). Vaccination with Pys25 alone had a weak but significant transmission-blocking effect compared with the effect observed for CT-vaccinated mice, suggesting that i.n. vaccination with the recombinant antigen alone might have some efficacy, even though the antibody levels for these two groups were not significantly different (Fig. 1). The oocyst prevalence was 100% for all vaccination regimens that we tested except both the passive and active Pys25-plus-CT regimens, for which the oocyst prevalence was 0% (Table 1). On the basis of our results, we concluded that i.n. vaccination with the malaria OSP was very efficacious when this OSP was combined with a mucosal adjuvant to block parasite transmission to mosquitoes.

DISCUSSION

Although most vaccines in use today are administered s.c. or intramuscularly, the advantages of mucosal vaccines are indisputable; they result in local immunity as well as systemic immunity, which, in general, is hard for parenteral vaccines to induce, and they provide a first line of defense against many infections that occur at or emanate from mucosal surfaces. They could prevent transmission of blood-borne pathogens by reuse of syringes; they may be safer and more cost-effective and thus have advantages for developing countries; and they are painless and therefore likely to be readily tolerated by small children and individuals with needle phobia (16). Although not all of the advantages attributed to mucosal vaccines mentioned above are directly relevant to the design of vaccines against malaria, and although there are some intrinsic technical difficulties that cannot be circumvented by development of effective mucosal vaccines (7), evaluation of the concept of designing mucosal vaccines for nonmucosal pathogens seems to be worthwhile.

To investigate malaria parasite OSP-based mucosal vaccines, we previously demonstrated that for two types of human malaria (*P. falciparum* malaria and *P. vivax* malaria) experimentally induced mouse immune sera specific for Pfs25 and Pvs25 (homologues of rodent Pys25) were very effective in blocking parasite transmission from patients' parasitized blood to mosquitoes in a membrane feeding assay (2, 3). In the present study we demonstrated that in a rodent malaria infection model, OSPs were immunogenic when they were administered i.n. (with levels of antigen-specific Igs reaching 15 mg/ml), and the induced immune serum was very effective in blocking parasite transmission. Most importantly, however, we demonstrated that vaccination directly prevented the transmission of a parasite from vaccinated animals to feeding mosquitoes. To our knowledge, this is the first demonstration that mucosal vaccination with malaria OSPs can directly prevent malaria transmission to mosquitoes in vivo. In the DBA/2 strain of mice lacking a component of the complement system, the number of oocysts formed is significantly increased in feeding mosquitoes (26); however, anopheline mosquitoes collected in field are usually not as heavily infected, and a single oocyst is commonly detected. Therefore, a more moderate antibody level may confer effective transmission-blocking immunity in humans (21).

Malaria vaccines targeting hepatic and erythrocytic stages suffer from antigenic variations mainly due to selection pressure from the host immune system. However, antigens expressed at a parasite sexual stage, such as OSPs, are immunologically concealed from the host immune system, and hence the chance that antigenic variations occur may be low. Indeed, OSPs of *P. falciparum* and *P. vivax* were shown to have minimal antigenic variations even in field isolates collected from remote regions of the world (19, 27). This is an important characteristic of ideal vaccines. On the one hand, sexual-stage antigens have disadvantages such as (i) the absence of an infection-induced booster effect and the resulting long-term immunity and (ii) the absence of direct protection of vaccinees from infection. Therefore, it is believed that a vaccine candidate should have multiple components and that at least one component should be a sexual-stage antigen (7). In such a vaccine formulation, preerythrocytic and/or erythrocytic antigens may function cooperatively with sexual-stage antigens for prevention of or reduction of infection and parasite transmission.

Mucosal administration, such as i.n. or oral administration, unlike parenteral immunization, of nonreplicating inert antigens with CT tends to induce Th2-type immunity, which is characterized by predominant induction of serum IgG1, induction of local secretory IgA, and in some cases induction of serum IgE in mouse models. Unlike what happens in other infectious diseases, which require induction of cell-mediated immunity (22), serum antibody, regardless of the Ig isotype, seems to be the predominant, if not only, protective arm of immunity that blocks malaria transmission. We do not know the mechanism of action of Pys25-specific antibodies in blocking parasite development in the midgut of a feeding mosquito, but binding of antibodies to the zygote surface and subsequent prevention of parasite development into the ookinete may be the most important blocking mechanism (14, 25). This antibody binding may occur within the midgut, and this may be independent of Ig isotypes. Thus, although IgE antibody is not the major antibody isotype present in a vaccinated host, it may contribute to blocking transmission. However, the induction of serum IgE may potentially lead to an allergic response in vaccinated individuals, and the data shown in Fig. 1b are relevant to this issue. Another important issue that needs to be

considered is the duration of protective antibodies. Recent findings relevant to the present work indicated that when *P. vivax* transmission-blocking vaccine candidate Pvs25 was injected s.c. with incomplete Freund's adjuvant into BALB/c mice, it induced a strong antigen-specific serum IgG response that was maintained for more than 6 months (our unpublished data). i.n. vaccination with Pvs25 plus CT induced a level of serum IgG comparable to that induced by s.c. vaccination formulated with incomplete Freund's adjuvant, but the level gradually decreased over 6 months. However, we found that i.n. vaccination with Pvs25 plus CT was generally more potent based on the magnitude and duration of the specific serum IgG response than s.c. vaccination with Pvs25 formulated with aluminum hydroxide (unpublished data).

In this study we used CT as a mucosal adjuvant; however, the use of CT for humans is hampered by the toxicity of this compound. Also, as mentioned above, issues related to the potential allergic response and the duration of antibodies need special consideration. Fortunately, however, nontoxic and thus safer adjuvants, but adjuvants that are as effective as CT, are being developed, making a mucosal malaria vaccine a feasible goal (1, 15). For example, we recently found that when a nontoxic subunit of CT, CTB, was fused to malaria OSP, it was efficacious by both the mucosal and s.c. routes for blocking parasite transmission (unpublished data). Thus, if the mucosal transmission-blocking vaccine efficacy data obtained with this rodent infection model can be reproduced in human clinical trials with guaranteed safety, OSP antigens formulated as noninvasive vaccines may become a powerful tool for use against human malaria.

ACKNOWLEDGMENTS

This work was supported by the Program of Founding Research Centers for Emerging and Reemerging Infectious Diseases of the Ministry of Education, Culture, Sports, Science and Technology (MEXT) of Japan. It was also supported in part by Grant-in-Aid for Scientific Research 18390129 from MEXT, Japan.

REFERENCES

1. **Agren, L. C., L. Ekman, B. Löwenadler, and N. Y. Lycke.** 1997. Genetically engineered nontoxic vaccine adjuvant that combines B cell targeting with immunomodulation by cholera toxin A1 subunit. J. Immunol. **158**:3936–3946.
2. **Arakawa, T., A. Komesu, H. Otsuki, J. Sattabongkot, R. Udomsangpetch, Y. Matsumoto, N. Tsuji, Y. Wu, M. Torii, and T. Tsuboi.** 2005. Nasal immunization with a malaria transmission-blocking vaccine candidate, Pfs25, induces complete protective immunity in mice against field isolates of *Plasmodium falciparum*. Infect. Immun. **73**:7375–7380.
3. **Arakawa, T., T. Tsuboi, A. Kishimoto, J. Sattabongkot, N. Suwanabun, T. Rungruang, Y. Matsumoto, N. Tsuji, H. Hisaeda, A. Stowers, I. Shimabukuro, Y. Sato, and M. Torii.** 2003. Serum antibodies induced by intranasal immunization of mice with *Plasmodium vivax* Pvs25 co-administered with cholera toxin completely block parasite transmission to mosquitoes. Vaccine **21**:3143–3148.
4. **Carter, R.** 2001. Transmission blocking malaria vaccines. Vaccine **19**:2309–2314.
5. **del Carmen Rodriguez, M., P. Gerold, J. Dessens, K. Kurtenbach, R. T. Schwartz, R. E. Sinden, and G. Margos.** 2000. Characterisation and expression of pbs25, a sexual and sporogonic stage specific protein of *Plasmodium berghei*. Mol. Biochem. Parasitol. **110**:147–159.
6. **Escalante, A. A., A. A. Lal, and F. J. Ayala.** 1998. Genetic polymorphism and natural selection in the malaria parasite *Plasmodium falciparum*. Genetics **149**:189–202.
7. **Genton, B.** 2008. Malaria vaccines: a toy for travelers or a tool for eradication? Expert Rev. Vaccines **7**:597–611.
8. **Gozar, M. M., O. Muratova, D. B. Keister, C. R. Kensil, V. L. Price, and D. C. Kaslow.** 2001. *Plasmodium falciparum*: immunogenicity of alum-adsorbed clinical-grade TBV25-28, a yeast-secreted malaria transmission-blocking vaccine candidate. Exp. Parasitol. **97**:61–69.
9. **Gozar, M. M., V. L. Price, and D. C. Kaslow.** 1998. *Saccharomyces cerevisiae*-secreted fusion proteins Pfs25 and Pfs28 elicit potent *Plasmodium falciparum* transmission-blocking antibodies in mice. Infect. Immun. **66**:59–64.
10. **Greenwood, B.** 2008. Can. malaria be eliminated? Trans. R. Soc. Trop. Med. Hyg. **103S**:S2–S5.
11. **Greenwood, B. M., D. A. Fidock, D. E. Kyle, S. H. Kappe, P. L. Alonso, F. H. Collins, and P. E. Duffy.** 2008. Malaria: progress, perils, and prospects for eradication. J. Clin. Investig. **118**:1266–1276.
12. **Hafalla, J. C., M. L. Santiago, M. C. Pasay, B. L. Ramirez, M. M. Gozar, A. Saul, and D. C. Kaslow.** 1997. Minimal variation in the Pfs28 ookinete antigen from Philippine field isolates of *Plasmodium falciparum*. Mol. Biochem. Parasitol. **87**:97–99.
13. **Harakuni, T., H. Kohama, M. Tadano, G. Uechi, N. Tsuji, Y. Matsumoto, T. Miyata, T. Tsuboi, H. Oku, and T. Arakawa.** 2009. Mucosal vaccination approach against mosquito-borne Japanese encephalitis virus. Jpn. J. Infect. Dis. **62**:37–45.
14. **Hisaeda, H., A. W. Stowers, T. Tsuboi, W. E. Collins, J. S. Sattabongkot, N. Suwanabun, M. Torii, and D. C. Kaslow.** 2000. Antibodies to malaria vaccine candidates Pvs25 and Pvs28 completely block the ability of *Plasmodium vivax* to infect mosquitoes. Infect. Immun. **68**:6618–6623.
15. **Holmgren, J., J. Adamsson, F. Anjuère, J. Clemens, C. Czerkinsky, K. Eriksson, C. F. Flach, A. George-Chandy, A. M. Harandi, M. Lebens, T. Lehner, M. Lindblad, E. Nygren, S. Raghavan, J. Sanchez, M. Stanford, J. B. Sun, A. M. Svennerholm, and S. Tengvall.** 2005. Mucosal adjuvants and anti-infection and anti-immunopathology vaccines based on cholera toxin, cholera toxin B subunit and CpG DNA. Immunol. Lett. **97**:181–188.
16. **Holmgren, J., and C. Czerkinsky.** 2005. Mucosal immunity and vaccines. Nat. Med. **11**:S45–53.
17. **Kaslow, D. C.** 1997. Transmission-blocking vaccines: uses and current status of development. Int. J. Parasitol. **27**:183–189.
18. **Kaslow, D. C., C. Bathurst, T. Lensen, T. Ponnudurai, P. J. Barr, and D. B. Keister.** 1994. *Saccharomyces cerevisiae* recombinant Pfs25 adsorbed to alum elicits antibodies that block transmission of *Plasmodium falciparum*. Infect. Immun. **62**:5576–5580.
19. **Kaslow, D. C., I. A. Quakyi, and D. B. Keister.** 1989. Minimal variation in a vaccine candidate from the sexual stage of *Plasmodium falciparum*. Mol. Biochem. Parasitol. **32**:101–103.
20. **Richie, T. L., and A. Saul.** 2002. Progress and challenges for malaria vaccines. Nature **415**:694–701.
21. **Saul, A.** 2008. Efficacy model for mosquito stage transmission blocking vaccines for malaria. Parasitology **135**:1497–1506.
22. **Seder, R. A., and A. V. Hill.** 2000. Vaccines against intracellular infections requiring cellular immunity. Nature **406**:793–798.
23. **Shi, Y. P., M. P. Alpers, M. M. Povoa, and A. A. Lal.** 1992. Single amino acid variation in the ookinete vaccine antigen from field isolates of *Plasmodium falciparum*. Mol. Biochem. Parasitol. **50**:179–180.
24. **Stowers, A. W., D. B. Keister, O. Muratova, and D. C. Kaslow.** 2000. A region of *Plasmodium falciparum* antigen Pfs25 that is the target of highly potent transmission-blocking antibodies. Infect. Immun. **68**:5530–5538.
25. **Tsuboi, T., Y. M. Cao, Y. Hitsumoto, T. Yanagi, H. Kanbara, and M. Torii.** 1997. Two antigens on zygotes and ookinetes of *Plasmodium yoelii* and *Plasmodium berghei* that are distinct targets of transmission-blocking immunity. Infect. Immun. **65**:2260–2264.
26. **Tsuboi, T., Y. M. Cao, M. Torii, Y. Hitsumoto, and H. Kanbara.** 1995. Murine complement reduces infectivity of *Plasmodium yoelii* to mosquitoes. Infect. Immun. **63**:3702–3704.
27. **Tsuboi, T., O. Kaneko, Y. M. Cao, M. Tachibana, Y. Yoshihiro, T. Nagao, H. Kanbara, and M. Torii.** 2004. A rapid genotyping method for the vivax malaria transmission-blocking vaccine candidates, Pvs25 and Pvs28. Parasitol. Int. **53**:211–216.
28. **Tsuboi, T., D. C. Kaslow, M. M. Gozar, M. Tachibana, Y. M. Cao, and M. Torii.** 1998. Sequence polymorphism in two novel *Plasmodium vivax* ookinete surface proteins, Pvs25 and Pvs28, that are malaria transmission-blocking vaccine candidates. Mol. Med. **4**:772–782.

Editor: W. A. Petri, Jr.

ELSEVIER

Journal of Hepatology 51 (2009) 333–341

Journal of Hepatology

www.elsevier.com/locate/jhep

Contribution of TIR domain-containing adapter inducing IFN-β-mediated IL-18 release to LPS-induced liver injury in mice☆

Michiko Imamura[1,2,3], Hiroko Tsutsui[2,*], Koubun Yasuda[3], Ryosuke Uchiyama[2], Shizue Yumikura-Futatsugi[3], Keiko Mitani[1], Shuhei Hayashi[2], Shizuo Akira[4], Shun-ichiro Taniguchi[5], Nico Van Rooijen[6], Jurg Tschopp[7], Tetsuya Yamamoto[8], Jiro Fujimoto[1], Kenji Nakanishi[3,9,*]

[1]*Department of Surgery, Hyogo College of Medicine, Nishinomiya, Japan*
[2]*Department of Microbiology, Hyogo College of Medicine, 1-1, Mukogawa-cho, Hyogo 663-8501, Nishinomiya, Japan*
[3]*Department of Immunology & Medical Zoology, Hyogo College of Medicine, Nishinomiya, Japan*
[4]*Department of Innate Immunity, Research Institutes for Microbiological Diseases, Osaka University, Suita, Japan*
[5]*Department of Molecular Oncology, Institute on Aging and Adaptation, Shinshu University, Graduate School of Medicine, Matsumoto, Japan*
[6]*Department of Cell Biology and Immunology, Free University, Amsterdam, The Netherlands*
[7]*Department of Biochemistry, University of Lausanne, Switzerland*
[8]*Department of Internal Medicine, Hyogo College of Medicine, Nishinomiya, Japan*
[9]*Collaborative Development of Innovation Seeds, Japan Science and Technology Agency, Tokyo, Japan*

***Background/Aims*: After treatment with heat-killed *Propionibacterium acnes* mice show dense hepatic granuloma formation. Such mice develop liver injury in an interleukin (IL)-18-dependent manner after challenge with a sublethal dose LPS. As previously shown, LPS-stimulated Kupffer cells secrete IL-18 depending on caspase-1 and Toll-like receptor (TLR)-4 but independently of its signal adaptor myeloid differentiation factor 88 (MyD88), suggesting importance of another signal adaptor TIR domain-containing adapter inducing IFN-β (TRIF). Nalp3 inflammasome reportedly controls caspase-1 activation. Here we investigated the roles of MyD88 and TRIF in *P. acnes*-induced hepatic granuloma formation and LPS-induced caspase-1 activation for IL-18 release.**

***Methods*: Mice were sequentially treated with *P. acnes* and LPS, and their serum IL-18 levels and liver injuries were determined by ELISA and ALT/AST measurement, respectively. Active caspase-1 in LPS-stimulated Kupffer cells was determined by Western blotting.**

***Results*: Macrophage-ablated mice lacked *P. acnes*-induced hepatic granuloma formation and LPS-induced serum IL-18 elevation and liver injury. *Myd88*$^{-/-}$ Kupffer cells, but not *Trif*$^{-/-}$ cells, exhibited normal caspase-1 activation upon TLR4 engagement *in vitro*. *Myd88*$^{-/-}$ mice failed to develop hepatic granulomas after *P. acnes* treatment and liver injury induced by LPS challenge. In contrast, *Trif*$^{-/-}$ mice normally formed the hepatic granulomas, but could not release IL-18 or develop the liver injury. *Nalp3*$^{-/-}$ mice showed the same phenotypes of *Trif*$^{-/-}$ mice.**

***Conclusions*: *Propionibacterium acnes* treatment MyD88-dependently induced hepatic granuloma formation. Subsequent LPS TRIF-dependently activated caspase-1 via Nalp3 inflammasome and induced IL-18 release, eventually leading to the liver injury.**

***Keywords*: Liver injury; LPS; IL-18; TRIF; Nalp3 inflammasome**

Received 6 January 2009; received in revised form 28 February 2009; accepted 12 March 2009; available online 20 May 2009
Associate Editor: C. Trautwein

☆ The authors who have taken part in this study declared that they do not have anything to disclose regarding funding from industry or conflict of interest with respect to this manuscript.

* Corresponding authors. Tel.: +81 798 456547/+81 798 456572; fax: +81 798 409162/+81 798 405423.
E-mail addresses: gorichan@hyo-med.ac.jp (H. Tsutsui), nakaken@hyo-med.ac.jp (K. Nakanishi).

Abbreviations: Ab, antibody; ASC, Apoptosis-associated speck-like protein containing a caspase recruitment domain; IL, interleukin; mAb, monoclonal antibody; MyD88, myeloid differentiation factor 88; Pro, precursor; TLR, Toll-like receptor; TRIF, TIR domain-containing adapter inducing IFN-β; WT, wild-type.

0168-8278/S36.00 © 2009 European Association for the Study of the Liver. Published by Elsevier B.V. All rights reserved.
doi:10.1016/j.jhep.2009.03.027